Carl von Ossietzky Universität Oldenburg

Deutsches Zentrum für Luft- und Raumfahrt
German Aerospace Center

Integrating Weather Forecast Uncertainty into Power Systems Management using the Probabilistic Power Forecast Evaluation Tool (ProPower)

Master Thesis in Engineering Physics

by

Hauke Mirco Bents

submitted to

First Supervisor	Prof. Dr. Carsten Agert
Second Supervisor	Dr. Lueder von Bremen

Oldenburg, 21st November 2023

Contents

List of Figures

List of Tables

Chapter 1

Introduction

Reducing global carbon dioxide emissions to net zero by 2050 is consistent with efforts to limit the long-term increase in average global temperatures to $1.5\,^{\circ}\mathrm{C}$. The path to net-zero emissions requires immediate deployment of clean and efficient energy technologies. The pathway of the International Energy Agency (IEA) calls for scaling up solar and wind power installment rapidly in the current decade. The installment of solar photovoltaics and wind power has to quadruple from 2020 until 2030. It is however expected, that low carbon emission technologies such as nuclear and hydro power will serve as an essential foundation for transitions (IEA, 2021).

Secure supply of electricity is essential for the prosperity of societies. It is expected that electricity will play a bigger role in heating, cooling, and transport, as well as in digitally integrated sectors such as finance and healthcare (IEA, 2021). A robust and secure supply of electricity is a prerequisite to functioning societies. The power sector has undergone significant changes, transitioning from centralized, vertically integrated systems that relied primarily n dispatchable thermal power plants to a system that features a diverse range of producers, many of whom utilize variable renewable energy (VRE) sources (IEA, 2020). Secure electricity systems should be able to supply demand under regular conditions, retain and return to regular conditions after disturbances and aim to absorb shocks. To improve on the accuracy of security assessments, planners and decision makers should develop probabilistic simulations of variability and interdependence of outcomes from their systems. Such an analysis could include VRE variability, outages of network components, system reserve margins and contingencies, load variability and many more (IEA, 2020). The European Network of Transmission System Operators for Electricity (ENTSOE-E) has recently engaged in probabilistic coordinated security assessment and risk management. The current focus is on comprehensive data collection of reliability data within the system operator community, and the development of a methodology to combine this data with data which is out of the operator's control (ENTSO-E, 2021).

There is an ongoing debate on how the requirement for electricity security could be realized in current electricity market designs. The purpose of future electricity markets may be considered from an economic, engineering or environmental-social-governmental perspective (Pinson, 2023). Fuel is no longer the only commodity to be allocated, and thus, prices should reflect on the need for security assets and support investments (IEA, 2022; Pinson, 2023). From a political and engineering perspective, it has to be defined what should or should not be handled through a market, and operational constraints are reflected in market clearing algorithms (Pinson, 2023). These constraints include for example market-clearing procedures constrained by power flow. A call to emphasize secure system operations is raised which should ensure the availability of relevant resources in case of contingencies. In recent research this has for example been addressed in security-constrained market-clearing approaches (Pinson, 2023). The optimal accommodation of flexible assets, such as energy storage, can be achieved by treating them as non-merchant assets, like the transmission system (Pinson, 2023).

Weather forecasts are applied at the heart of these processes. Deterministic numerical weather forecasts (NWP) have improved steadily due to advances in numerical solution schemes and parametrizations schemes for subgrid scales, the access to more observation data including satellites as well as increases in computational power (Bauer et al., 2015; Sweeney et al., 2019). The development of probabilistic forecasts, and of very short-term forecasts are expected to have a great impact on system planning processes and near-delivery time operations. Historically, probabilistic forecasts have emerged to quantify the uncertainty which is inherent to forecasting non-linear dynamic systems. Recently, they have for example been employed in forecasting wind power ramp events. These events become more and more important as wind penetration increases (Sweeney et al., 2019). The most relevant information to use in power systems is power production on timescales from minutes to a few hours ahead. Statistical models based on recent observations have emerged due to high computational expenses for data assimilation and NWP modeling which may already be out-of-date when computations are finished. Augmentation of power production data with remote sensing is an established technique for improving solar power forecasts. Both satellite imagery and sky cameras are of use for intra-hour forecasting (Sweeney et al., 2019). In wind power forecasting, LIDAR and RADAR technologies are being employed to observe and model wind speed fields as they approach wind farms (Theuer et al., 2020).

It has been shown by Morales et al. (2014) that dispatch decisions based on pure deterministic forecasts lead to sub-optimal market clearing. To overcome this issue, they proposed a stochastic market clearing model. In this model, average balancing costs are estimated from a set of scenarios of renewables feed-in that are equivalent to ensemble members from an ensemble prediction system.

This work will evaluate the added value of probabilistic forecasts and short-term forecasts in a sequential market clearing setup using the probabilistic power forecast evaluation tool (ProPower) (Schyska, 2021). The day-ahead market clearing optimizes the dispatch of wind farms and conventional generators based on day-ahead forecasts from the European Center for Medium Range Weather Forecasts (ECMWF). A second market clearing (intraday) has been implemented which is based on updated forecasts of higher skill. The amount of required balancing is determined by the deviation of forecasted renewables feed-in to feed-in computed from ERA5 reanalysis data.

Theory of ensemble forecasting, electricity markets and economic dispatch is given in section 2. The deterministic and stochastic day-ahead and intraday clearing methods are described. ProPower is introduced in section 3 together with a description of model networks and associated sensitivity studies. Section 4.1 compares the deterministic and stochastic day-ahead clearing methods on a simple two-node network. Section 4.2 applies the method to a five-node network and discusses sensitivity studies on flexibility and cost parameters. Conclusions and an outlook are given in section 5.

Chapter 2

Theory

2.1 Ensemble Forecasting

Ensemble forecasting is a method to quantify the range of uncertainty when predicting the future state of the atmosphere. Generally, the forecast uncertainty is comprised of initial condition errors and model errors.

Numerical weather prediction systems and the atmosphere can be considered as non-linear dynamic system whose evolution depends on the initial conditions. However, the estimates of the current state of the atmosphere are inaccurate as they are bound to observation deficiencies and errors from numerical assimilation techniques. Forecast models on the other hand are subject to numerical inadequacies due to truncation errors or limitations in parametrizations of sub-grid scale processes (e.g. cumulus formation) (Leutbecher & Palmer, 2008).

Advances in model accuracy have, to some extent, been driven by the increase in high-performance computing resources as this allows to resolve higher spatial resolution models which then caption smaller scales of motion. These advances are however still limited by the entanglement of initial condition error and model errors. The initial condition error can be studied when comparing the model outcomes for a given time step obtained from model runs initialized with a time lag. Figure 2.1 compares the root-mean-squared error of the unperturbed control forecast of the ECMWF EPS (represented by the heavy line) with the RMS difference of two subsequent (12-h) lag control forecasts valid at the same time (represented by the thin line). In the review of Leutbecher and Palmer (2008) on ensemble forecasting, the difference of lagged forecasts is taken as an estimate of the forecast error due to initial conditions. If the heavy line is an estimate of the actual RMS error of the 500 hPa geopotential height forecast, then the difference between both line can be attributed to the forecast errors from model errors. According to this analysis, the growth of initial errors over time appears to cause a large fraction of the forecast errors, i.e. represented by the thin line.

Ensemble forecasting has emerged as a technique to encapsulate the growth of initial condition uncertainties and errors arising from imperfect model formulations. It aims at predicting the

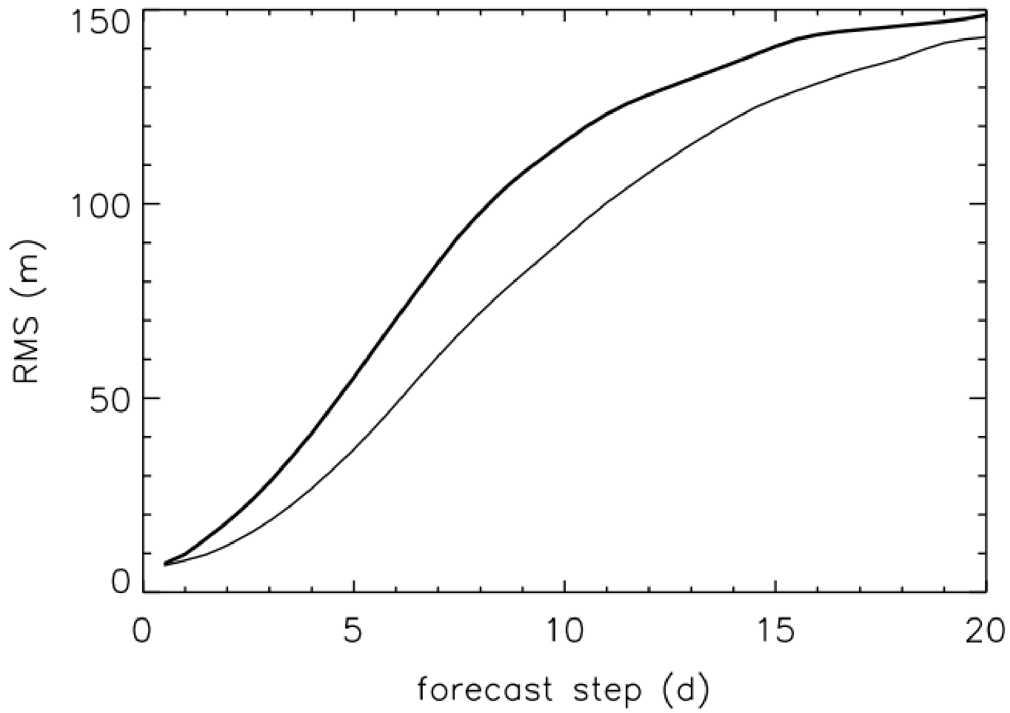

Figure 2.1: 500 hectopascal geopotential height RMS error (heavy line) of the unperturbed control forecast of the ECMWF EPS and RMS difference of two subsequent (12-h lag) control forecasts valid at the same time (thin line). Reproduced from Leutbecher and Palmer (2008) with permission from Elsevier

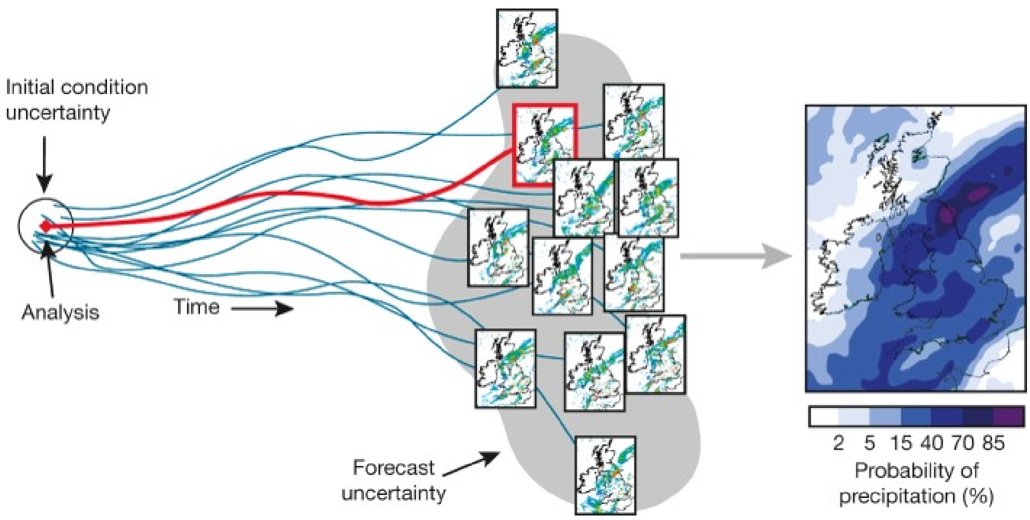

Figure 2.2: Schematic diagram of 36-h ensemble forecasts used to estimate the probability of precipitation over the UK. Reproduced from Bauer et al. (2015) with permission from Springer Nature.

probability density state of the atmosphere at a future time in a quantitative manner. The numerical weather prediction problem is of non-linear complexity which means that purely statistical methods to assign an uncertainty to the forecast are inadequate, as they do not provide a reliable representation of the model spread. Instead, an ensemble of many realizations of the system is required. This concept is illustrated in figure 2.2. It shows how a 36-h ensemble of forecasts which is used to estimate the probability of precipitation over the UK. Each realization is produced starting from slightly different initial conditions to account for imperfections in the assessment of the current state of the Earth system, and with perturbed models to account for approximations in the simulation (Bauer et al., 2015).

In practice, these realizations are referred to as ensemble members which are created by adding perturbations to the initial state and to the physical processes in the model (Bauer et al., 2015). These solutions (ensemble members) provide a sample of the forecast uncertainty. Several statistical methods have emerged to determine these perturbations. First studies have been carried out using Monte-Carlo methods which are technically expensive to run due to the large number of required members. Today, large weather prediction models make use of the Breeding Vector method, the Ensemble Kalman Filter method, and the Singular Vector method (R. J. Bessa et al., 2017; Leutbecher & Palmer, 2008).

A brief remark shall be given to the value of the ensemble mean over an unperturbed forecast. The RMS error of an ensemble mean is generally lower than that of an unperturbed forecast as the unpredictable scales of motion have been filtered in the ensemble mean and only the signal of the predictable scales remain (Leutbecher & Palmer, 2008).

The skill of an ensemble forecast is estimated through its reliability and resolution. The reliability of a forecast considers the statistical consistency (reliability) of the predicted probabilities and the resolution measures the width of the distribution. The statistical consistency is defined upon the closeness of the predicted probability and measured relative frequency of an event. The resolution of a forecast addresses the issue that a broad reliable distribution may be considered less useful than a narrow predicted distribution which resolves better whether an event is likely to occur or not. The continuous ranked probability skill score measures both reliability and resolution (Leutbecher & Palmer, 2008).

It is expected from theory, that given a large sample size of events, the forecast ensemble mean error tends to the ensemble mean spread times a factor close to 1. This implies that the forecast spread can be used to predict the standard deviation of the mean forecast error distribution (Leutbecher & Palmer, 2008). Transferring this discussion to real prediction models, we are not dealing with perfect ensembles. At high prediction horizons, RMS error and RMS spread correlate well for large sample sizes. For short forecast ranges (up to two days), the spread is less reliable in prediciting the variability of the width of the ensemble mean error distribution. For cases with large (small) ensemble spread, the average RMS error is systematically lower (higher) than the spread (Leutbecher & Palmer, 2008). Calibration and improvements of the initial uncertainty representation and model uncertainty representation are expected to lead to significant improvements of the statistical consistency (Leutbecher & Palmer, 2008).

2.1.1 Probabilistic forecast evaluation

To handle probabilistic forecasts, it is useful to employ simple and robust measures which provide information on location, spread or symmetry of the data set. The location refers to the central tendency or general magnitude of the data. The spread denotes the degree of variation or dispersion around the central value. Symmetry describes the balance with which the data values are distributed about their center (Wilks, 2019).

Common measures for location and spread of a given sample are the mean and standard deviation. Measures based on quantiles are simple to obtain and robust against outliers. The sample quantile q_p is a number with the same units as the data, which exceeds the proportion of the data given by the subscript p, with $p \in [0, 1]$ (Wilks, 2019). The median $q_{0.5}$ is a measure for the location and is the central value of a sorted data set. The lower and upper quartiles $q_{0.25}$ and $q_{0.75}$ can be interpreted as the central values of the lower and upper half of the sorted data set. The difference between both is referred to as the inter-quartile range $\mathrm{IQR} = q_{0.75} - q_{0.25}$ which is a simple measure for the spread of the data set. It simply specifies the range of the central 50% of the data (Wilks, 2019). The median, and the lower and upper quartile commonly define the box in a simple box-whisker plot which is used to interpret probabilistic forecast data.

2.2 Economic management of power systems

2.2.1 Electricity markets

The energy commerce between producers and consumers is generally available in two different trading ranges, the electricity pool and the futures market. The pool is a market place where energy is traded on a short-term basis. It accommodates a day-ahead market, and several adjustment markets. The futures market place accommodates electricity trading on medium- to long-term horizons. Additionally, the option of signing bilateral contracts between suppliers and consumers is available (Conejo et al., 2010). Reserve and regulation markets are cleared to provide stand-by power as spinning and non-spinning reserves which are activated in the case of strong disruptions of supply (i.e. network failures, generator outage or strong changes in intermittent energy generation).

This work focuses on the sequential stages in the energy pool namely day-ahead market, and the intraday markets, which handle a majority of energy transactions. In 2021, Germany's overall electricity consumption amounted to 504.5 TWh. Of this, 200 TWh were cleared in the day-ahead market, and 67 TWh were cleared in intraday markets[1]. The intraday volume has increased by 33 TWh since 2015. The balancing energy has so far remained constant around 1.4 and -1.6 TWh[2].

[1] Traded volume on the EPEX Day-ahead and Intraday for the year 2021. Intraday volume resolved to up and down corrections not available, https://www.epexspt.com/en/tradingproducts, accessed 29th October 2023.

[2] Data for the *Ausgleichsenergie* in 2021, post-processed by the German Bundesnetzagentur, https://www.smard.de/home/marktdaten, accessed 29th October 2023.

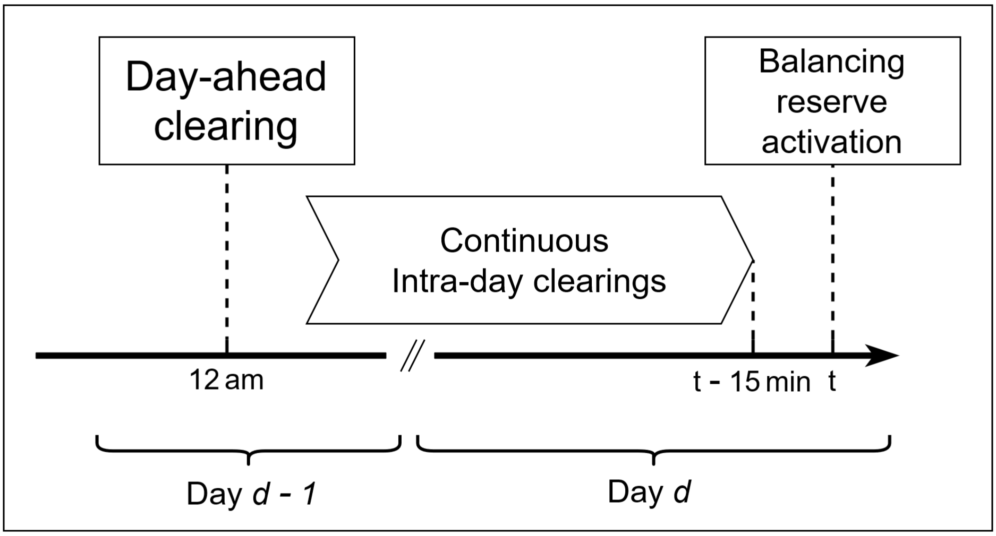

Figure 2.3: The German electricity market design with the day-ahead and intraday markets for energy trade. Reserve markets have been omitted as they are not available in ProPower. The balancing reserve (i.e. primary, secondary and tertiary frequency regulation) is activated at delivery t.

Both day-ahead and intraday markets are organized as auctions where market participants submit energy blocks and their minimum selling price for every hour of the market horizon. Retailers and consumers submit energy blocks and their maximum buying prices for every hour of the market horizon as well. Offers and bids are collected by the market operator which then clears the market using a market-clearing procedure. Traditionally, a deterministic procedure is employed in which the offers are accepted starting from the cheapest costs. Accepted offers are paid according to the price of the most costly accepted offer.

The day-ahead market clearing yields production and consumption schedules (Conejo et al., 2010), which are also referred to as dispatch. The clearings of the intraday auctions yield positive and negative corrections to the day-ahead dispatch. Positive and negative corrections to the day-ahead schedule dispatch are treated differently. They correspond to purchases and repurchases of energy at the market. This work will discuss day-ahead market-clearing procedures in the sections 2.3.1 and 2.3.3, and intraday procedures in the sections 2.3.4 and 2.3.5.

In Germany[3], the dispatch of day d has been cleared on the day-ahead market of the previous day $d-1$ at 12:00. The dispatch applies from 00:00 until 23:00 in hourly resolution which means that the VRE forecast of the earliest dispatch is 12 hours old, and 35 hours old for the latest. Afterwards, there are intraday auctions every quarter hour starting at 15:00 with a lead time of 5 minutes. Take for example a delivery at 18:00, then the last intraday adjustment for the block between 18:00 and 18:15 is cleared at 17:55.

[3]The German spot markets is operated in the EPEX SPOT – European Power Exchange which organizes the day-ahead and intraday trade for multiple countries across Europe, https://www.epexspot.com/en/powermarketbasics, accessed 29th October 2023.

After the last intraday auction for some delivery time t has closed, the system operator controls the dispatch of generators. At delivery, balancing reserves of a network region may be activated to ensure the stability of the network frequency. The frequency containment reserve or primary reserve must be operational within 30 s to prevent wide-spread black-out quickly. The automatic and minute frequency regulation reserves (i.e. secondary and tertiary reserves) are activated afterwards if the primary reserve was not sufficient to contain the mismatch between demand and supply.

In Europe, the primary reserve requirements are settled by a group of associated transmission system operators, while the secondary and tertiary reserves are being settled by each system operator independently through auctions. In Germany, a market for reserve power and energy is cleared on an hourly basis before delivery. It is defined to cover for both generation excess and deficit. It is the last market prior to power delivery. When auctions are cleared, single or two-price schemes define based on regulation direction and position of the producer / consumer whether they pay or receive the balancing market price (Klæboe & Fosso, 2013).

2.2.1.1 Management of Uncertainty

In electricity markets, uncertainty includes the availability of production units and network components, power production for non-dispatchable producers (e.g. wind and solar power plants, prices for energy and power markets, demand of consumers and retailers) (Conejo et al., 2010). Research on this type of uncertainty splits into two perspectives. The generator and consumer side is concerned with the uncertainty of their supply and demand, as well price uncertainties and implications on their actions. Uncertainty of supply and demand are of importance to transmission system operators as they have to ensure a stable supply of electricity to the population. This work focuses on the system operators perspective. From a market participants perspective, uncertainty affects trading decisions most. Producers, consumers, retailers and non-dispatchable producers can participate in different stages of the electricity market. The level of day-ahead, adjustment, reserve market prices poses a key uncertainty in trading decisions. A theoretical foundation for the modeling of such decisions has been laid out in the work of Conejo et al. (2010) for producers, non-dispatchable producers and consumers. Considering the example of a wind farm operator, the volatility of day-ahead, intraday and imbalance prices on the one hand and intermittent wind power production on the other hand serve as an input to the problem of placing optimal bids. A model (Kraft et al., 2023) was discussed where the trading decisions of a trader are based on three decision stages (balancing reserve market, day-ahead spot market, and intraday spot market). When characterizing uncertainty information available to the trader solely through risk-neutral optimization (i.e. maximization of the expected profit) one cannot capture the full depth of the information. Depending on the risk level of the operator, uncertainty information may be used to reduce losses or maximize profits when trading in sequential electricity market. Risk-hedging strategies for example secure profits on earlier stages, gaining independence from intraday price volatility.

A comprehensive analysis (Hirth & Ziegenhagen, 2015) on the German intraday and reserve market has discussed three possibilities of interaction between variable renewables and the balancing system: the impact on reserves, participation of renewable generators on balancing markets, and the incentives provided by imbalance settlement scheme. It was found that although installed photovoltaic and wind power generation capacity has tripled from 2008 until 2015, balancing reserves have reduced by 15% and costs for balancing power has reduced by 50%. Furthermore, it was pointed out that wind and solar power forecast errors are only one of several important factors which determines the balancing reserve requirements. The structure of the balancing power market and the imbalance settlement scheme has been highlighted as crucial catalysts for the requirement of balancing reserves. Further work has been carried out on analyzing that taking long- or short-positions in trading systematically is not expected to generate benefits in the current imbalance settlement scheme (Koch & Hirth, 2019).

The system operators perspective aims at maximizing social welfare instead of maximizing individual profits. In principle, this is obtained by reducing fuel consumption of generators and reducing loss of supply to consumers. The market clearing process has been named above as the central process of the market or system operator to clear offers and bids by market participants. These bids are inherently influenced by uncertainty information available to market participants, but the clearing result is driven by stochastic processes (e.g. weather). If the wind speed forecast for a given time is low, then less wind power is cleared in general. Updates and improvements by short-term weather forecasts determine the clearing of energy corrections in the intraday markets.

Conventionally, the day-ahead and balancing markets are settled independently. Stochastic producers are typically cleared considering their expected production at very low marginal cost. Energy adjustments required to cope with associated forecast error are left to the flexible units participating in the balancing market. If not enough flexible capacity is provided, balancing costs may escalate (Morales et al., 2014). Two strategies are suitable to solve this challenge. The first one is to establish reserve markets, where the reserve demand is specified by the transmission system operator. The reserve is then made available to the balancing mechanisms at delivery. The second suitable, and more recent, approach to handle the need for flexibility aims at optimizing the dispatch of flexible generators more efficiently using stochastic optimization (Zheng et al., 2015) is to clear the day-ahead market using stochastic optimization. Deterministic clearing models assume the next day situation to be fixed, while stochastic models include uncertainties. The day-ahead dispatch can be optimized to minimize expected total costs by anticipating balancing needs from a probabilistic forecast (Morales et al., 2014). Alternatively, the day-ahead dispatch could also be optimized to minimize the costs associated with the worst case scenario (Zheng et al., 2015).

Without the claim to completeness, two studies should be highlighted which carried out interesting investigation on the modeling of sequential electricity market clearing. The first study (Zhou et al., 2012) employed a two-settlement electricity market with clearing of day-ahead and real-time markets for energy and operating reserves. In the day-ahead clearing, a deterministic point forecast is input to the unit commitment and dispatch procedure. A probabilistic forecast was used to adjust the commitment status of flexible units closer to real time, based on either dynamic operating reserves or stochastic unit commitment. The real-time dispatch was based on the realized availability of wind power. It was found that probabilistic forecasts can contribute to improve the performance of the power system, both in terms of cost and reliability.

The second study (Morales et al., 2014), which large parts of this work are based upon, uses a two-stage optimization problem for the optimization of day-ahead dispatch under consideration of anticipated balancing requirements from probabilistic forecasts. Reserve requirements are being determined without the need of input from outside (i.e. the TSO). The stochastic dispatch optimization of day-ahead decisions was presented as the most efficient method compared settling day-ahead and balancing markets separately. It was however noted, that the stochastic dispatch optimization may lead to producers being cleared in a loss-making position.

So far, studies have mostly concentrated on simple forecast scenarios or purely statistical approaches to predicting wind energy. Power forecasts have been deduced from Beta distributions in Morales et al. (2014), representative scenarios post-processed from real-world measurements have been used in Conejo et al. (2010). Probabilistic forecast have also been generated from forecast error distribution based on the copula theory, using the auto-regressive integrated moving average (ARIMA) method, employing artificial neural networks, or using kernel density estimation (Ahmed & Khalid, 2019; R. Bessa & Matos, 2010; Zhou et al., 2012). The use of ensemble forecasts has so far been recommended but not carried out (R. J. Bessa et al., 2017; Zheng et al., 2015).

2.2.2 Economic dispatch problem

From a system perspective, the electricity market is cleared at several stages prior to delivery from day-ahead to intraday. A preliminary operational schedule for all generators is generally established from load and generation forecasts in the day-ahead clearing. In this work perfect foresight is assumed for the demand side while renewable generation is modeled more explicitly. This process is also referred to as an *economic dispatch* or *unit commitment problem* depending on the technical resolution. It is the mathematical optimization problem of scheduling generators under the goal of cost minimization.The day-ahead and intraday market clearings are implemented as an *economic dispatch problem* in this work. As both unit commitment and economic dispatch are employed throughout literature, this section shall briefly discuss the difference. In summary, economic dispatch simplifies generator constraints such as start-up, shut-down, ramp-up, and -down constraints which may be imposed over a longer duration of time (i.e. spanning over multiple hours). Network constraints, on the other hand, are usually not included in the regular unit commitment problem (Conejo & Baringo, 2017).

The planning horizon of both unit commitment and economic dispatch is usually 24 hours. The objective of the unit commitment problem is to determine the scheduling of generating units that is needed to minimize total costs, supply the demand, and meet the different technical constraints of generators (e.g. multi-hour ramping, off-times) and security requirements for the supply of demand. Generating units have associated costs that are the sum of no-load or fixed costs, variable costs, start-up costs and shut-down costs. Generators are associated with ramping limits above which power cannot be increased in between two time steps. The system adheres to total power balance, i.e. the sums of demand and supply have to at least equalize. The problem may be formulated with security constraints in the form of required power reserves per time step (Conejo & Baringo, 2017).

The economic dispatch problem in comparison is defined by the objective to determine the output power per generating unit which satisfies the demand at minimum variable cost while solely complying with dispatch limits of generating units. The solution is trivial without a network as generators are scheduled with respect to their costs. In reality, network constraints limit the flow through power lines. Economic dispatch with network constraints then optimizes the power output of generating units to satisfy demand, simplified generator constraint (e.g. ramping per time step) and network constraints for a single period of time (Conejo & Baringo, 2017).

2.3 Implementation of market clearings

Remarks on notation

The power system scheduling and operation is modeled in three separate stages (day-ahead clearing, intraday clearing, and balancing measures) with results from one stage being used as inputs to the subsequent stage. Inputs to a clearing stage shall be generally given in upper case letters while outputs of the clearing stage are denoted in lower case letters.

Example: Generating dispatch schedule in day-ahead clearing as output g. Compared to optimized generating dispatch schedule in intraday clearing or for balancing at delivery as input G.

The second convention used in this work is used in stochastic optimization problems to distinguish between first and second decision stage variables. Second stage variables are denoted with a subscript ω.

Example: Anticipated balancing corrections per scenario ω in the stochastic day-ahead clearing $g_\omega^{+/-}$ in contrast to balancing corrections during balancing at delivery $g^{+/-}$.

The third convention is used to differentiate between upwards ($+$) and downwards ($-$) corrections. These are found in the stochastic day-ahead and intraday clearing, as well as the balancing. Variables for corrections measures are derived from the day-ahead dispatch variable g by adding a superscript $+$ or $-$ corresponding to the direction of correction. Parameters (e.g. costs or ramping limits) associated with the correction measures are defined accordingly.

Example: Upwards balancing measures g^+ to a generators dispatch may not exceed the share η^+ of their nominal capacity $\bar{G}$. The cost of correction is the marginal cost $C_{n,s}$ increased by an cost extra for purchases κ^+.

A fourth convention used in this work distinguishes between vectors and scalars. A vector containing the same type of information for a range of elements is displayed in bold font in contrast to a scalar element from this vector which is represented by normal font.

Example: The deterministic day-ahead cost function $\mathcal{C}^{\mathrm{DA}}$ takes the operating cost and the power dispatch per generator as an input. The vector of all operating costs over all generators is displayed as **C** with the cost for an individual generator at node n with carrier s being defined as $C_{n,s}$.

2.3.1 Deterministic day-ahead clearing

The power system is described by a set of buses $\mathcal{N}$. These buses $n \in \mathcal{N}$ are connected by lines denoted with index $l \in \mathcal{L}$. Each bus is assigned with an inelastic electricity demand time series $D_{n,i,t}$ per load sector $i \in \mathcal{I}$. This load can be served by electricity generation from a set of generators installed at the respective bus $s \in \mathcal{S}_n$. The generation itself is bound to costs, the operating (or marginal) costs of the generator $C_{n,s}$. These are assumed to be time-independent. The generation is limited by the installed nominal power of the generator $\bar{G}_{n,s}$ and by the availability of the power source, which may vary in time $\tilde{G}_{n,s,t}$ (weather dependent).

Transmission lines distribute energy between buses, where it is generated, and the buses, where it is consumed. The connection pattern is defined by the adjacency matrix $K_{n,l}$. Lines are assigned with a nominal capacity $\bar{f}_l$. We assume at time t that the transmission of electricity is not bound to operating costs. The flow along line l is denoted with $f_{l,t}$. The definition of the optimization problem follows largely the style and formulations of (Brown et al., 2018; Schyska, 2021).

$$\mathcal{C}^{\mathrm{DA}}(\boldsymbol{C}, \boldsymbol{g}(t)) = \sum_{n,s} C_{n,s} g_{n,s,t} \tag{2.1}$$

A generation schedule $g_{n,s,t}$ is optimized for every generating unit in the system for the time horizon of 24 to 47 hours ahead. Equation 2.1 describes the day-ahead operating costs resulting from a generation schedule. To optimize the generation schedule, a linear optimization problem is formulated that minimizes the operating costs. It is defined in the set of equations 2.2.

$$\min_{g(t), f(t)} \mathcal{C}^{\mathrm{DA}}, \forall t \tag{2.2a}$$

The optimization is subject to the following constraints:

1. At any node n and at any time step t generation g and exports f have to match the demand D (**nodal balancing**):

$$\sum_s g_{n,s,t} - \sum_l K_{n,l} f_{l,t} = \sum_i D_{n,i,t}, \forall n, t \tag{2.2b}$$

2. Generation g may not exceed available capacity at any time.

$$g_{n,s,t} \leq \tilde{G}_{n,s,t} \cdot \bar{G}_{n,s} \tag{2.2c}$$

3. Variable bounds

$$0 \leq g_{n,s,t} \tag{2.2d}$$

$$0 \leq |f_{l,t}| \leq \bar{f}_l \tag{2.2e}$$

The resource availability $\tilde{G}_{n,s,t}$ in equation 2 is different for conventional generators (later defined as e.g. gas turbines or nuclear power stations) and stochastic generators (i.e. wind farms). It is assumed that conventional generators are constantly available and down-times due to external effects such as maintenance are not modeled. Stochastic generators on the other hand can only be dispatched up to their forecasted availability provided in hourly resolution. We assume perfect foresight for the demand, hence $D_{n,i,t}$ is known.

In the day-ahead auction, producers are scheduled according to their marginal costs. Renewable generators, and wind farms in particular, are assumed to have very low or zero marginal cost (Morales et al., 2014). Given a deterministic forecast, renewable generators are therefore scheduled first, up to their forecasted capacity, the remaining demand is then fulfilled by conventional generators ranked by their marginal costs.

2.3.2 Balancing measures

The balancing reserve activation is modeled to occur at delivery. Here, adaptations to the day-ahead dispatch become necessary due to deviations between observed availability of stochastic generators $\tilde{O}_{n,s,t}\bar{G}_{n,s}$ and the day-ahead dispatch $G_{n,s,t}$. We assume that this mismatch can be balanced by flexible producers (similar to (Morales et al., 2014)). These flexible producers are assumed to provide an instantaneous ramp up or reduction $g^{+/-}_{n,s,t}$ in their generation. They receive cost premiums for modifications to their day-ahead dispatch as defined in equations 2.3a, 2.3b. In the case of positive corrections required by the system, generators charge a cost extra κ^+ from the system operator. In the case of negative corrections required (i.e. DA dispatch of conventional generator too high if observation exceeds forecast) the flexible generator re-purchases capacity from the system operator at a discount κ^- (Morales et al., 2014). In a sense, this is also a cost extra, when assuming that a flexible generator is willing to repurchase capacity at a discount with respect to the offer used in the day-ahead clearing, i.e. the keeping some of the income received in the day-ahead clearing (Morales et al., 2014).

Additional flexibility is offered by stochastic producers curtailing their production. The most costly balancing measure is shedding of load (Morales et al., 2014). Keeping these balancing measures small, maximizes social welfare (Schyska, 2021).

The cost of balancing is the sum of costs for corrections performed by flexible generators as well as the cost of load shedding as defined in equation 2.3c. A cost-optimal set of balancing measures is obtained by minimizing the total cost $\mathcal{C}^{\mathrm{BM}}$ function.

$$C^{+}_{n,s} = (1 + \kappa^{+}_{n,s}) \cdot C_{n,s} \tag{2.3a}$$

$$C^{-}_{n,s} = (1 - \kappa^{-}_{n,s}) \cdot C_{n,s} \tag{2.3b}$$

$$\mathcal{C}^{\mathrm{BM}}\left(\boldsymbol{C}^{+/-}, \boldsymbol{C}^{shed}, \boldsymbol{g}^{+/-}(t), \boldsymbol{s}(t)\right) = \sum_{n,s}\left(C^{+}_{n,s} g^{+}_{n,s,t} + C^{-}_{n,s} g^{-}_{n,s,t}\right) + \sum_{n,i}\left(C^{shed}_{n,i} s_{n,i,t}\right) \tag{2.3c}$$

$$\min_{g^{+/-}(t), s(t), f(t)} \mathcal{C}^{\mathrm{BM}}, \ \forall t \tag{2.4a}$$

The optimization of balancing measures is subject to the physical and technical constraints:

1. Nodal balancing has to be fulfilled at every node n at any time step t given the required corrections $g^{+/-}_{n,s,t}$. An auxiliary load shedding variable $s_{n,i,t}$ is included to ensure feasibility of the constraint.

$$\sum_{s}\left(g^{+}_{n,s,t} + g^{-}_{n,s,t}\right) - \sum_{l} K_{n,l} f_{l,t} + \sum_{i} s_{n,i,t} = \sum_{i} D_{n,i,t} - \sum_{s} G_{n,s,t}, \ \forall n, t \tag{2.4b}$$

2. The sum of the corrections and day-ahead dispatch per node n, generator s and time step t should not exceed the observed availability $\tilde{O}_{n,s,t}$.

$$g^{+}_{n,s,t} + g^{-}_{n,s,t} \leq \tilde{O}_{n,s,t} \bar{G}_{n,s} - G_{n,s,t} \tag{2.4c}$$

3. A generator may only provide flexibility up to a certain share η of its nominal capacity.

$$0 \geq g^{-}_{n,s,t} \geq -\eta^{-}_{n,s} \bar{G}_{n,s} \tag{2.4d}$$

$$0 \leq g^{+}_{n,s,t} \leq \eta^{+}_{n,s} \bar{G}_{n,s} \tag{2.4e}$$

4. For technical feasibility, balancing measures are limited by scheduled and nominal capacity.

$$g^{-}_{n,s,t} \geq -G_{n,s,t} \tag{2.4f}$$

$$g^{+}_{n,s,t} \leq \bar{G}_{n,s} - G_{n,s,t} \tag{2.4g}$$

5. Shedding may not exceed given load and power flow per line may not exceed nominal link capacity.

$$0 \leq s_{n,i,t} \leq D_{n,i,t} \tag{2.4h}$$

$$0 \leq |f_{l,t}| \leq \bar{f}_{l} \tag{2.4i}$$

2.3.3 Stochastic day-ahead clearing

It has been previously shown by (Morales et al., 2014) that separating the decisions made in the day-ahead clearing from future balancing reserve activations may lead to non-optimal market clearings. In the deterministic case, the day-ahead clearing does not account for uncertainty in forecasts and potential balancing costs can therefore not be anticipated. Consider now, that the power production of a stochastic generator is predicted by a finite set of scenarios Ω where each scenario ω is characterized by a vector of power values $g_{n,s,t,\omega}$ with a probability of occurrence π_ω. Probabilistic weather forecasts, e.g. provided by ECMWF, fulfill these criteria with each member giving a scenario of equal probability (Leutbecher & Palmer, 2008).

In the deterministic case, day-ahead clearing and balancing reserve activation were considered as independent which is in fact not completely true, as the day-ahead solution enters the balancing market as a parameter. The stochastic day-ahead model combines both decision stages into a bi-level optimization problem where the day-ahead dispatch $g_{n,s,t}$ is now being optimized under consideration of potential balancing measures $g^{+/-}_{n,s,t,\omega}$ for each scenario $\omega \in \Omega$ (observe added expectation value in 2.6a).

The costs for balancing are being estimated depending on the anticipated purchase and repurchase actions, as well as shedding measures per scenario ω as defined in 2.5.

$$\begin{aligned}\mathcal{C}^{\mathrm{BM}}\left(\boldsymbol{C}^{+/-}, \boldsymbol{C}^{shed}, \boldsymbol{g}^{+/-}(t,\omega), \boldsymbol{s}(t,\omega)\right) = &\sum_{n,s}\left(C^{+}_{n,s}g^{+}_{n,s,t,\omega} + C^{-}_{n,s}g^{-}_{n,s,t,\omega}\right) \\ &+ \sum_{n,i}\left(C^{shed}_{n,i}s_{n,i,t,\omega}\right)\end{aligned} \tag{2.5}$$

To optimize the day-ahead dispatch of generators, the day-ahead operating cost and the expected balancing costs have to be minimized as defined in the optimization problem 2.6.

$$\min_{g(t), f(t,\omega), g^{+/-}(t,\omega), s(t,\omega)} \mathcal{C}^{\mathrm{DA}} + \sum_{\omega\in\Omega} \pi_\omega \cdot \mathcal{C}^{\mathrm{BM}}(\omega),\ \forall t \tag{2.6a}$$

Constraints formulated for the stochastic optimization ensure nodal balancing and technical feasibility both at the day-ahead as well as after balancing for every scenario. The constraints 1 – 2.2e for the conventional day-ahead objective function 2.1 are being complemented with constraints from the balancing market for every scenario. These are

1. Nodal balancing under consideration of day-ahead dispatch and anticipated balancing measures for every feed-in scenario.

$$\sum_s \left(g^{+}_{n,s,t,\omega} + g^{-}_{n,s,t,\omega}\right) - \sum_l K_{n,l} f_{l,t,\omega} + \sum_i s_{n,i,t,\omega} + \sum_s g_{n,s,t} = \sum_i D_{n,i,t} \tag{2.6b}$$

2. Generation may not exceed its maximum capacity for both conventional and stochastic generators (Morales et al., 2014).

$$0 \leq g_{n,s,t} \leq \bar{G}_{n,s} \tag{2.6c}$$

3. Corrections should not exceed the availability of generation. The forecasted availability $\tilde{G}_{n,s,t,\omega}$ of stochastic generators is defined per scenario ω. The availability of conventional

generators is unchanged.

$$g^{+}_{n,s,t,\omega} + g^{-}_{n,s,t,\omega} + g_{n,s,t} \leq \tilde{G}_{n,s,t,\omega}\bar{G}_{n,s} \tag{2.6d}$$

4. Maximum ramping down should not exceed the capacity scheduled in the day-ahead clearing.

$$g^{-}_{n,s,t,\omega} \geq -g_{n,s,t} \tag{2.6e}$$

5. Balancing measures of generators may not exceed the share η of their nominal capacity.

$$0 \geq g^{-}_{n,s,t,\omega} \geq -\eta^{-}_{n,s}\bar{G}_{n,s} \tag{2.6f}$$

$$0 \leq g^{+}_{n,s,t,\omega} \leq \eta^{+}_{n,s}\bar{G}_{n,s} \tag{2.6g}$$

6. Flow through lines is limited by the link capacity and shedding may not exceed the given demand.

$$0 \leq s_{n,i,t,\omega} \leq D_{n,i,t} \tag{2.6h}$$

$$0 \leq |f_{l,t,\omega}| \leq \bar{f}_l \tag{2.6i}$$

2.3.4 Deterministic intraday clearing

Intraday clearing offers adjustments or corrections $g^{+/-,*}$ to the dispatch before delivery. It gives producers the opportunity to adjust their day-ahead dispatch based on updated and improved forecasts. Producers are expected to have lower costs for corrections in the intraday clearing than during balancing at delivery. The cost benefit is represented by a premium factor $\varrho \in [0,1]$ which is multiplied to reduce the premium for balancing (see equations 2.7a, 2.7b). Upwards and downwards corrections are expected to be more flexible This is represented by a factor $K \geq 1$ which is multiplied on the share $\eta^{+/-}$ of nominal capacity defining a generators flexibility. The operating costs for intraday corrections are defined in 2.7c

$$C^{+,*}_{n,s} = (1 + \varrho \cdot \kappa^{+}_{n,s}) \cdot C_{n,s} \tag{2.7a}$$

$$C^{-,*}_{n,s} = (1 - \varrho \cdot \kappa^{-}_{n,s}) \cdot C_{n,s} \tag{2.7b}$$

$$\begin{aligned}\mathcal{C}^{\mathrm{ID}}\left(\boldsymbol{C}^{+/-,*}, \boldsymbol{C}^{\mathrm{shed}}, \boldsymbol{g}^{+/-,*}(t), \boldsymbol{s}(t)\right) = &\sum_{n,s}\left(C^{+,*}_{n,s} g^{+,*}_{n,s,t} + C^{-,*}_{n,s} g^{-,*}_{n,s,t}\right) \\ &+ \sum_{n,i} C^{\mathrm{shed}}_{n,i} s_{n,i,t}\end{aligned} \tag{2.7c}$$

A cost-optimal set of intraday corrections is achieved by minimizing the resulting operating costs under given technical constraints (see problem 2.8)

$$\min_{g^{+/-,*}(t), f(t), s(t)} \mathcal{C}^{\mathrm{ID}} \tag{2.8a}$$

Constraints of the intraday clearing are comparable to those for the balancing measures.

1. Nodal balancing under consideration of intraday corrections.

$$\sum_s \left(g^{+,*}_{n,s,t} + g^{-,*}_{n,s,t}\right) - \sum_l K_{n,l} f_{l,t} + \sum_i s_{n,i,t} = \sum_i D_{n,i,t} - \sum_s G_{n,s,t} \tag{2.8b}$$

2. The sum of the corrections and day-ahead dispatch must not exceed the updated, forecasted availability.

$$(g^{+,*}_{n,s,t} + g^{-,*}_{n,s,t}) \leq \tilde{G}_{n,s,t}\bar{G}_{n,s} - G_{n,s,t} \tag{2.8c}$$

3. Upwards corrections must not exceed a generators maximum capacity. Downwards corrections must not exceed day-ahead dispatch.

$$g^{+,*}_{n,s,t} \leq \bar{G}_{n,s} - G_{n,s,t} \tag{2.8d}$$

$$g^{-,*}_{n,s,t} \geq -G_{n,s,t} \tag{2.8e}$$

4. Generators may provide more flexibility $K \cdot \eta$ compared to the share available for balancing.

$$0 \geq g^{-,*}_{n,s,t} \geq -K \cdot \eta^{-}_{n,s}\bar{G}_{n,s} \tag{2.8f}$$

$$0 \leq g^{+,*}_{n,s,t} \leq K \cdot \eta^{+}_{n,s}\bar{G}_{n,s} \tag{2.8g}$$

5. Load shedding may not exceed a given load and power flow through lines is limited by the link capacity.

$$0 \leq s_{n,i,t} \leq D_{n,i,t} \tag{2.8h}$$

$$0 \leq |f_{l,t}| \leq \bar{f}_l \tag{2.8i}$$

2.3.5 Stochastic intraday clearing

Following the fashion of introducing a stochastic day-ahead dispatch which is optimized under anticipation of balancing measures, a stochastic formulation of the intraday clearing is presented. Costs for corrections are defined equivalent to the deterministic intraday clearing (see equation 2.7), however the optimization problem now minimizes cost for corrections $\mathcal{C}^{\text{ID}}$ and the expected balancing costs as introduced in the stochastic day-ahead optimization (see equation 2.5).

$$\min_{g^{+/-,*}(t), g^{+/-}(t,\omega), s(t,\omega), f(t,\omega)} \mathcal{C}^{\text{ID}} + \sum_{\omega \in \Omega} \pi_\omega \cdot \mathcal{C}^{\text{BM}}(\omega),\ \forall t \tag{2.9a}$$

A feasible solution is achieved by adhering to a set of constraints 2.6b, 2.6d and 2.6e, previously introduced in the stochastic day-ahead clearing. However, as the day-ahead dispatch has already been settled, the dispatch is relabeled as $g_{n,s,t} \rightarrow G_{n,s,t}$.

1. Nodal balancing under consideration of balancing measures for every feed-in scenario.

$$\begin{aligned}\sum_i D_{n,i,t} - \sum_s G_{n,s,t} = &\sum_s \left(g^{+,*}_{n,s,t} + g^{-,*}_{n,s,t}\right) \\ &- \sum_l K_{n,l} f_{l,t,\omega} \\ &+ \sum_s \left(g^{+}_{n,s,t,\omega} + g^{-}_{n,s,t,\omega}\right) \\ &+ \sum_i s_{n,i,t,\omega} \end{aligned} \tag{2.9b}$$

2. The sum of the corrections, anticipated balancing measures and day-ahead dispatch must not exceed the updated, forecasted availability per scenario.

$$\left(g^{+,*}_{n,s,t} + g^{-,*}_{n,s,t}\right) + \left(g^{+}_{n,s,t,\omega} + g^{-}_{n,s,t,\omega}\right) \leq \tilde{G}_{n,s,t,\omega}\bar{G}_{n,s} - G_{n,s,t} \tag{2.9c}$$

3. Downwards corrections must not exceed day-ahead dispatch. Upwards corrections must not exceed a generators maximum capacity.

$$g^{-,*}_{n,s,t} \geq -G_{n,s,t} \tag{2.9d}$$

$$g^{+,*}_{n,s,t} \leq \bar{G}_{n,s} - G_{n,s,t} \tag{2.9e}$$

4. Balancing measures of generators may not exceed some share η of their nominal capacity.

$$0 \geq g^{-}_{n,s,t,\omega} \geq -\eta^{-}_{n,s}\bar{G}_{n,s} \tag{2.9f}$$

$$0 \leq g^{+}_{n,s,t,\omega} \leq \eta^{+}_{n,s}\bar{G}_{n,s} \tag{2.9g}$$

5. Generators may provide more flexibility $K \cdot \eta$ compared to the share available at balancing.

$$0 \geq g^{-,*}_{n,s,t} \geq -K \cdot \eta^{-}_{n,s}\bar{G}_{n,s} \tag{2.9h}$$

$$0 \leq g^{+,*}_{n,s,t} \leq K \cdot \eta^{+}_{n,s}\bar{G}_{n,s} \tag{2.9i}$$

6. Load shedding may not exceed the given demand and flow through lines is limited by the link capacity.

$$0 \leq s_{n,i,t,\omega} \leq D_{n,i,t} \tag{2.9j}$$

$$0 \leq |f_{l,t,\omega}| \leq \bar{f}_l \tag{2.9k}$$

Chapter 3

Methodology

3.1 Preparation of wind power forecast and observation

The preparation of wind power forecasts requires two basics steps. Meteorological data such as the wind speed are retrieved from a numerical weather prediction system in the first step. The resulting power output is obtained form a wind-to-power-model. In this work, the wind-to-power model was a power curve of a single Vestas V164/9500 offshore wind turbine[1] with a rated power output of 9.5 MW, cut-in at 3 m/s and cut-out wind speed at 25 m/s. The wind speed has been converted to capacity factors instead of absolute power values to allow for scaling of wind farm nominal capacity. Wake effects are not represented in this simple model.

Ensemble forecast data by the European Centre for Medium-Range Weather Forecasts (ECMWF) has been acquired in hourly resolution for the year 2021. The data set contains 50 members and was not calibrated before. ECMWF reanalysis data (short ERA5) has been used as observation. The preparation of input data was carried out by my colleague Lueder von Bremen. In this work, the data for eight different sites in the West and North-West of Germany have been processed. Three offshore sites and five onshore sites have been considered as shown in table 3.1.

[1] Technical data from Open Energy Platform (OEP), https://openenergy-platform.org/dataedit/view/supply/wind_turbine_library, accessed 5. June 2023

Name	Type	Location	Capacity Factor
Büttel	onshore	(53.90°N, 9.23°E)	24.6%
Hohe See	offshore	(54.34°N, 7.22°E)	50.3%
Marienhafe	onshore	(53.35°N, 7.22°E)	31.6%
Sandbank	offshore	(55.06°N, 7.23°E)	49.7%
Wilhelmshaven	onshore	(53.56°N, 8.09°E)	27.3%
Nordergründe	offshore	(53.82°N, 8.12°E)	38.6%
Hamburg	onshore	(53.53°N, 10.01°E)	20.5%
Ruhrgebiet	onshore	(51.51°N, 7.23°E)	20.1%

Table 3.1: List of locations for retrieval of meteorological data. Capacity factors calculated from ERA5 data for 2021.

Exemplary Forecast and Observation Data

Figure 3.1 shows the day-ahead predicted capacity factor of a windfarm over 24 hours. It shows a wind ramp over six hours from 10% to 90% median feed-in. The full view of ensemble members shown as grey lines provides detailed information over the ensemble but is rather difficult to interpret. Therefore, it the data has been abstracted as described in section 2.1.1. The inter-quartile range (represented by the dark blue shaded area) features 50% of forecast members, the median (represented by dark blue line) is the central tendency of the ensemble.

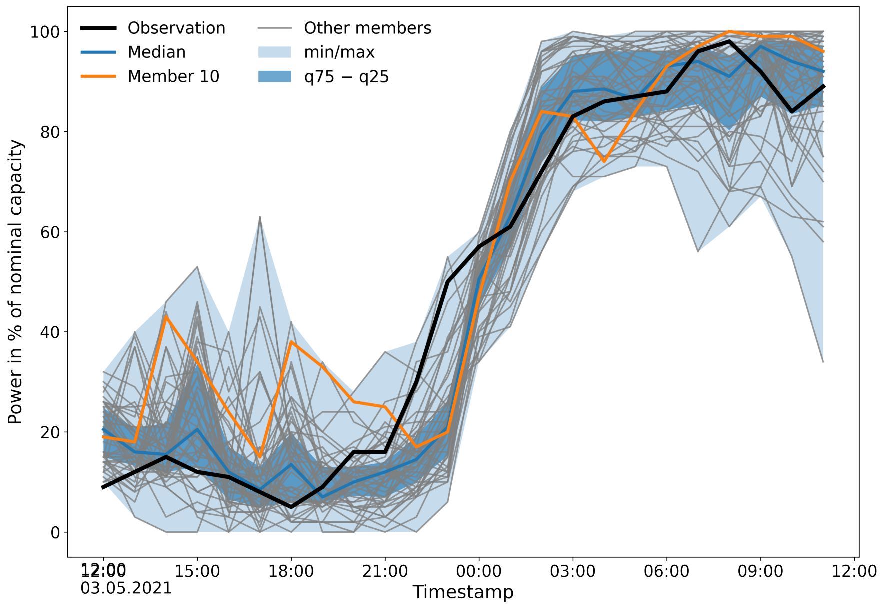

Figure 3.1: Illustration of the day-ahead capacity factor forecast of the wind farm *onwind Büttel* over a day in hourly resolution derived from ECMWF EPS data. A spaghetti plot of all 50 members in grey is shown, the inter-quartile range and median highlighted in dark blue. The deterministic forecast ($\omega = 10$) is highlighted in orange line and the ERA5 observation data is shown in black.

While the full ensemble is used for stochastic market clearing, only member 10 (represented by the orange line) is chosen as the deterministic forecast in the deterministic market clearing.

3.2 ProPower – Probabilistic Power Forecast Evaluation Tool

3.2.1 Model structure

The probabilistic power forecast evaluation tool (ProPower) is a Python package which provides the framework to simulate market clearing procedures as described in section 2.2.2. It has been implemented by my colleague Bruno Schyska as part of his dissertation (Schyska, 2021). The basic structure has been derived from the open-source package *Python for Power System Analysis (PyPSA)*. PyPSA stores all data about network components in DataFrame objects of the Python library *Pandas*. This allows for simple and fast indexing of the data. Optimization problems are formulated using the Python-based optimization modeling language *Linopy* (Brown et al., 2018; Hofmann, 2023). Linopy is an open-source Python package to build and process linear and mixed-integer optimization with *n*-dimensional labeled input data. It outperforms the common alternative Pyomo in both memory requirements and initialization time (Hofmann, 2023). In ProPower, all operations are performed on the `StochNetwork` object which replaces the network object from PyPSA by including a further dimension besides time steps to represent members from probabilistic forecasts.

Three different stages of modeling have been implemented into ProPower which have already been discussed in 2.2.1 for the electricity market in general. The continuous intraday clearing have been simplified to one clearing per time step in the day-ahead dispatch (see fig. 3.2).

The day-ahead clearing has been implemented into two functions. The initialized network object, as well as time steps called *snapshots* serve as inputs to the `deterministic_day_ahead` function. The `stochastic_day_ahead` function requires forecast *members* in addition to that. The frequency, as well as start and end time are defined by the *snapshots* as they serve as the index of all DataFrames. A time series of the optimized day-ahead dispatch for every generator is stored in the network object.

The intraday markets as described in section 2.2.1, are represented by a single intraday clearing procedure. It is cleared once per time step. Sine stochastic generators receive 15-minute ahead forecasts, the clearing is placed 15 minutes before delivery. The clearing is implemented by the two functions `stochastic_intraday_market` and `deterministic_intraday_market`. A time series of the optimized intraday corrections for every generator is stored in the network object. These corrections are then added onto the day-ahead dispatch schedule to update it.

Lastly, the balancing reserve activation is modeled with the function `balancing_market`. It is assumed to be operating at near-real time as the final stage after day-ahead and intraday clearing. It has been designed to balance out deviations between (updated) dispatch and observed feed-in, taking the *observed* power feed-in from stochastic generators as input.

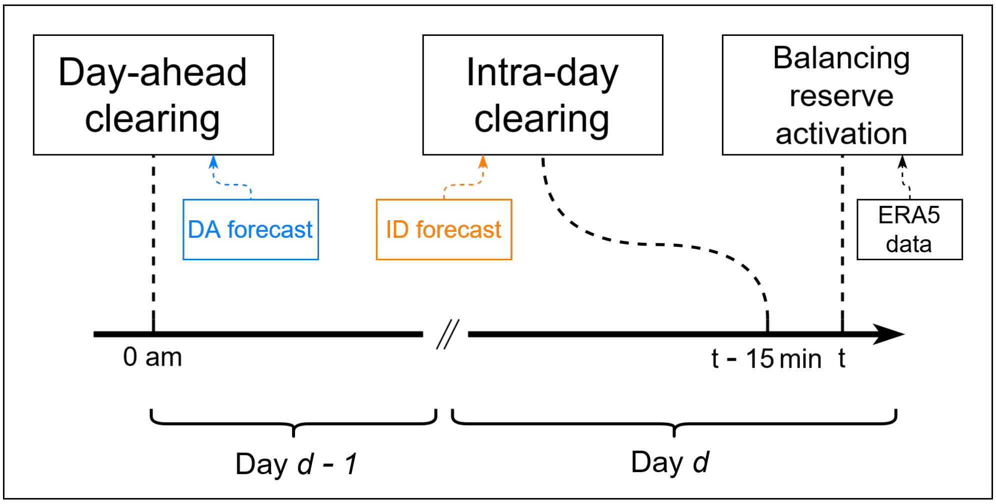

Figure 3.2: Day-ahead clearing based on 24-hour ahead forecasts, an intraday clearing with 15-minute ahead forecasts, and balancing reserve activation with ERA5 reanalysis data is being modeled in ProPower.

3.2.2 Framework for simulations

As ProPower itself is just the framework for simulations, one has to set up scripts which define the concrete application. In the case of this thesis, six different wrapper functions have been built which pre-process and feed the data into the tool, and finally export the simulation results into some post-processing. The wrappers also define the loop over months and days as the optimization of a full year in a single problem is too large.

These basic functions have been explained in table 3.2. Function 1 is employed to import forecasts and observation data which is then used to initialize the network object with function 2. Function 3 performs the day-ahead and balancing optimization for the given network on a single day. The optimization of intraday corrections may be included optionally. This configuration of market clearings is then repeated over the days per month using function 5. The results from day-ahead, intraday and balancing clearing are stored using function 4. A loop over all months in the year 2021 is then defined in function 6 where parallel handling of months may be specified.

In general, three different sets of input data have to be prepared, which results in eight (or eleven including meteorological data) different output time series. Every optimization requires an input network, defined through files for the buses (or *nodes*) and links, load time series and associated shedding costs per load sector, technical details on generators, and the range of snapshots for the model. The structure has been adapted from PyPSA. From the set of generators, the stochastic generators then receive day-ahead forecast and observation data as an input. If intraday clearing shall also be simulated then the day-ahead forecasts are replaced by a set of intraday forecasts. Input and output directories, the day-ahead clearing method, the intraday clearing option, the forecast member chosen as deterministic forecast, intraday premium ϱ and extra flexibility K, as well as cost extras κ^+ and κ^- are defined in the config file.

Function	Description
(1) read_forecasts	INPUT: Path to forecast file, frequency of forecast OUTPUT: pandas.DataFrame with forecast data Reads ensemble forecast from file; interpolation to 15 minutes as an option
(2) initialise_network	INPUT: config-array, network directory, forecast data OUTPUT: propower.StochNetwork object Initializes network from files with probabilistic or deterministic (single member) forecast and observations
(3) clear_markets	INPUT: config-array, network object, list of snapshots, list of members, intraday forecasts, solver name OUTPUT: Updated network object 1. Computes deterministic or stochastic day-ahead clearing 2. Solution is clipped and stored to network-object 3. Optional intraday clearing with stochastic or deterministic intraday function add solution onto day-ahead dispatch 4. Compute balancing measures from day-ahead dispatch and observations 5. Store results in network object
(4) export_to_csv	INPUT: config-array, network object OUTPUT: CSV-Files for Generators: p_day_ahead, p_intraday_up, p_intraday_down, p_balancing_up, p_balancing_down; Links: p0, Loads: p_set, shedding, Wind: forecasted_p_max_pu, observed_p_max_pu Exports data stored in network object
(5) clear_and_get	INPUT: config-array, month, days in month, frequency of forecast, solver name OUTPUT: Calls export_to_csv, list of infeasible days 1. Loops over days per month and imports forecasts (DA and ID) and observations for all windparks 2. Calls initialise_network 3. Calls clear_markets 4. Defines paths for outputs and calls export_to_csv
(6) main	INPUT: Path to config file 1. Loads config file 2. Defines IO and specifies parallelization 3. Loops over months per year 4. Gets days per month and calls clear_and_get

Table 3.2: Central subroutines for the simulation of market clearings. Network topologies are stored in a network directory. The clearing sequence is stored in the config-file.

3.3 Design of power network topology

Two network topologies have been used in this study. A two-node network allows for isolated analysis of the interplay between market design and forecast data. An extended five-node network additionally includes the influence of network constraints as well as more realistic load profiles.
Networks are stored in the standard format recommended by PyPSA (Brown et al., 2018). Both networks feature flexible (e.g. gas turbines) and inflexible (e.g. hard coal or nuclear power plants) conventional generators. Both networks also feature stochastic generators in the form of on- and offshore wind farms. Meteorological forecast and reanalysis data is used as a source for power feed-in forecast and observation.

3.3.1 Two-node network

The two-node network has been adapted from the simple demonstrator introduced in the work of Morales et al. (2014). The network captures a simple interplay between conventional generator scheduling and stochastic feed-in. Three conventional generators with varying marginal costs are featured. G1 is the second largest, but the most expensive generator at 35 €/MWh (see table 3.3). It is flexible at a cost extra of 14% for upwards corrections and 3% for downwards corrections, and thus, they can be used for balancing. G2 and G3 are cheaper but inflexible.

The installed wind capacity is 16.1% and the share of flexible generation is 32.3% of total installed generation capacity. The system load is constant with 80 MW installed at bus 1 and 90 MW at bus 2. The link capacity is 100 MW.

Generator WP receives probabilistic forecasts and observation data of the location Nordergründe.

		Bus 1			Bus 2
		G1	G2	WP	G3
$\bar{G}$	(MW)	100	110	50	50
C	(€/MW h)	35	30	0	10
κ^+	(%)	14	–	–	–
κ^-	(%)	3	–	–	–
η^+	(%)	20	–	100*	–
η^-	(%)	40	–	100	–

Table 3.3: Generator data of two-node network adapted from Morales et al. (2014). *WP cannot be increased beyond its observed feed-in.

3.3.2 Five-node network

The extended network is made of five nodes connected with five links which are located in the West and North-West of Germany (see figure 3.3). This region already faces high penetration of wind feed-in at the moment which is expected to rise in the future. Conventional and stochastic production units are installed at every node. Stochastic feed-in is only represented by wind power plants. Strong links are placed from Emsland *Ems* and Hamburg (*HH*) to the

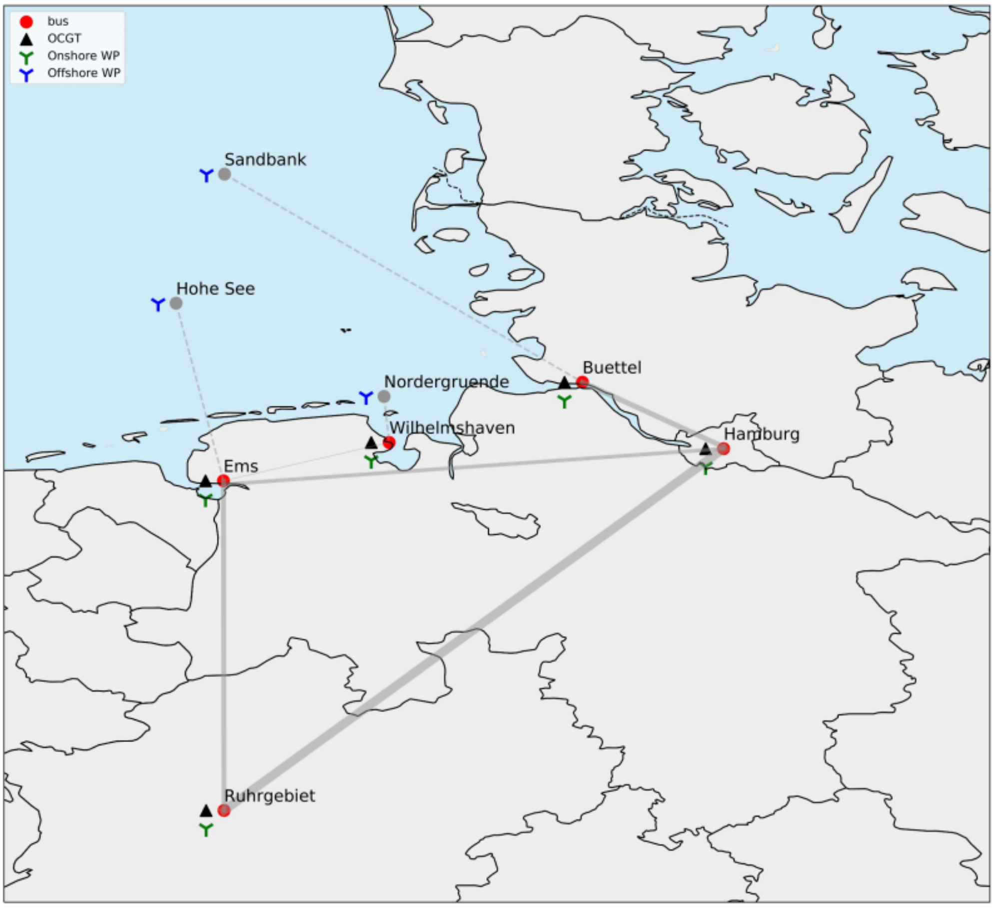

Figure 3.3: Five-node network situated in the northwest of Germany with stochastic / renewable feed-in from wind farms and conventional power production from inflexible and flexible units at every bus. The network incorporates both onshore and offshore wind conditions. The demand is defined per node and associated with three different load sectors. The network has been developed in cooperation with Buller (2023) who gave the permission to reproduce this visualization.

Ruhrgebiet (*Ruhr*) as they will serve as a central corridor to transmit offshore wind power to hubs of demand in the South.

The demand per node has been defined in three steps. First, the annual demand of Hamburg and Ruhrgebiet was defined. Secondly, the demand of Emsland, Wilhelmshaven (*WHV*) and *Buettel* has been defined depending on this. Thirdly, temporal demand profiles for the year 2021 have been defined using the annual demand per sector and bus.

The annual electricity demand per node and sector is shown in table 3.5. Openly available annual electricity demand data of German States was taken from the Open Energy Platform (OEP) for Hamburg and Ruhrgebiet as a reference[2]. The demand categories *Domestic*, *Commercial-Trade-Services (CTS)* and *Industry* have been adopted as well. The demand of the remaining nodes has been defined depending on Hamburgs demand (see table 3.4) to represent places with rural characteristics, i.e. low total demand. Hamburg and Ruhrgebiet serve as demand

[2]Electricity consumption of the German federal states in 2011 from OEP, https://openenergy-platform.org/dataedit/view/demand/ego_demand_federalstate, accessed 5. June 2023

hubs. Cost of shedding per load sector is specified in table 3.6. The CTS shedding cost is based on the cost from Morales et al. (2014). Industrial load shedding is supposed to be preferable, and thus, cheap. Load profiles for every bus were generated using standard load profiles which have been deposited in *demandlib*[3].

$\tilde{d}$	Buettel	HH	Ems	WHV	Ruhr
HH	0.1	**1**	0.15	0.3	9.6

Table 3.4: Ratio of demand allocated per bus $\tilde{d}$ to the demand allocated in Hamburg.

	Sector	Buettel	HH	Ems	WHV	Ruhr
$\sum_t D_t$ (GWh)	Domestic	514.4	3821.0	449.3	910.6	30202.9
	CTS	403.3	3994	505.6	1024.9	26360.0
	Industry	339.0	4678	891.4	1807.0	63682.0
	Σ	1256.7	12493.0	1846.3	3742.5	120244.9

Table 3.5: Total annual electricity demand per node divided into three different demand sectors. The demand data for HH and Ruhr have been taken from the OEP data set.

Sector	C_{shed} (€/MW)
Domestic	250
CTS	200
Industry	150

Table 3.6: Shedding cost C_{shed} associated with electricity demand from the three available sectors.

Generator capacity per node and type of generator is shown in table 3.7. Available carriers (i.e. generator types) are defined in tab. 3.8. Conventional generation can be covered by flexible open-cycle-gas-turbines (*OCGT*) and inflexible nuclear power plants (*nuclear*). Renewable generation is covered by wind farms. OCGT and nuclear generators are also referred to as conventional generators. Stochastic generator is used to refer to renewable generators as their power output is defined by stochastic processes (Morales et al., 2014).

Conventional generators are installed at every node with a capacity to cover the corresponding peak demand at that node. The nominal capacity of onshore wind farms was defined relative to the total annual electricity demand per node and a capacity factor deduced from meteorological time series introduced above (see tab. 3.1). Buettel, Emsland, and Wilhelmshaven are designed to cover 500, 350, and 150% of their annual electricity demand through onshore wind power, respectively. In contrast to that, Ruhrgebiet and Hamburg cover 9 and 2% of their annual demand with onshore generation. Offshore wind farm capacity is defined relative to the annual demand of Hamburg. Hohe See (*offshore Ems*) should cover 250% of Hamburg's annual demand, Sandbank (*offshore Buettel*) 150% and Nordergründe (*offshore Wilhelmshaven*) is designed to cover 15% of Hamburg's demand.

Link capacities, i.e. upper power transmission limits to links, are shown in table 3.9. Strong links connect Hamburg and Ruhrgebiet, as well as Ems and Ruhrgebiet. Weaker links interconnect

[3]BDEW Electricty Load Profiles, https://demandlib.readthedocs.io/en/latest/bdew.html#electrical-profiles, accessed 5. June 2023

	Carrier	Buettel	HH	Ems	WHV	Ruhr	Σ
	Conventional	216.3	2122.0	305.6	620.6	19280.1	22544.6
$\bar{G}$ (MW)	Onshore	2853.9	114.2	2561.6	2568.5	5707.8	13806.0
	Offshore	4280.8	–	7134.7	428.1	–	11843.6

Table 3.7: Nominal capacity of generators installed per bus in five-node network.

Carrier		C (€/MWh)	κ^+ (%)	κ^- (%)	η^+ (%)	η^- (%)
conventional	OCGT	4.5	14	3	20	40
	Nuclear	2.6	–	–	–	–
stochastic	On-/Offshore	0	–	–	100*	100

Table 3.8: Technical details of reference configuration of available generators in the model. Costs adapted from PyPSA's technology data base (Victoria et al., 2023). *Wind farms cannot feed-in beyond their observed availability.

the Northern part of the network. Offshore wind farms are connected via sufficiently large links, and are therefore modeled as if they were located directly at the respective connecting node.

$\bar{f}_{ij}$ (MW)	Buettel	HH	Ems	WHV	Ruhr
Buettel	–	3567	0	0	0
HH		–	2539	0	6106
Ems			–	428	3347
WHV				–	0
Ruhr					–

Table 3.9: Nominal capacity of links between buses in five-node network.

3.4 Sensitivity analysis on the five-node network

3.4.1 Share of flexible generators

The difference between stochastic and deterministic clearing on the five-node network (see section 3.3.2) with 100% flexible conventional generation has already been covered by Buller (2023). To study the impact of short-term forecasts in the proposed market clearing (see section 3.2) scheme, a further study on the same five-node network configuration has been carried out. Here, it was found that the reduction of total costs, load shedding and curtailment through the integration of short-term forecasts is small (see section 4.2).

A sensitivity analysis has been designed to quantify the added value of short-term forecast information if the installed flexible generation capacity is varied. The share of flexible generators in the total installed conventional generation capacity was varied from 0 to 100% in eleven steps (see table 3.10). This parameter is also referred to as the *flexible* or *OCGT* share. The network configurations where used in four different clearing sequences. Deterministic and stochastic day-ahead clearing were modeled, and balancing measures were obtained with and without prior intraday clearing. ECMWF EPS 24 to 48 hour ahead forecasts of 2021 were used as day-ahead forecasts and 15-minute ahead forecasts served as a basis for the intraday clearing. ERA5 reanalysis data was used as an observation for balancing measures. 8760 time steps for

Flexible share (%)	$\sum_n \bar{G}_{n,\text{OCGT}}$ (MW)	$\sum_n \bar{G}_{n,\text{nuclear}}$ (MW)
0	0	22544.6
10	2254.5	20290.1
20	4509.0	18035.6
30	6763.4	15781.2
40	9017.8	13526.8
50	11272.3	11272.3
60	13526.8	9017.8
70	15781.2	6763.4
80	18035.6	4509.0
90	20290.1	2254.5
100	22544.6	0

Table 3.10: The total installed generation capacity over all buses $\sum_n \bar{G}_{n,s}$ for flexible OCGTs and inflexible nuclear generators for eleven different flexible shares.

every hour of the year were modeled. The cost extras from table 3.3 were used. The intraday premium factor $\varrho = 0.8$ and extra intraday flexibility $K = 1.2$ were used.

So called key indicators were employed to estimate the significance of the impact of installed flexible generation capacity on the dispatch and balancing in general. Five indicators were investigated with respect to the flexible share. The results are presented in section 4.2.1.1 where the indicators are defined in detail.

1. Total annually averaged system operating costs $\langle \mathcal{C}_{\text{total}} \rangle_t$
2. Total annual conventional day-ahead dispatch E_s per carrier $s \in \{\text{OCGT}, \text{nuclear}\}$
3. Total annual amount of shedded demand E^{shed}
4. Total annual curtailment of wind farms $E^{\text{curtailed}}$
5. Total annual intraday corrections $E^{+/-,*}$

3.4.2 Impact of costs for balancing measures

The costs at the balancing stage are comprised of both the costs for load shedding, as well as the costs for adjusting flexible generators. The stochastic day-ahead dispatch is optimized to reduce expected balancing costs, and should therefore be affected by the input costs. In the current setup ($\kappa^+ = 14\%$ and $\kappa^- = 3\%$), it is generally cheaper to procure flexible capacity in the day-ahead clearing as it is expected to be expensive in the balancing. How do total costs and shedding change when expected upwards balancing costs decrease?

The cost extra for purchase measures κ^+ and the cost discount for repurchase measures κ^- have been varied from (14% / 3%) to (3% / 14%) in twelve steps (see table 3.11), following the assumption that total system costs will remain unaffected, as positive and negative errors between forecast (ensemble) and observation should occur with the same relative frequency. For this analysis, only the ratio of purchase to repurchase cost extras was of interest and therefore the up-to-down ratio R was introduced (see eq. 3.1). The five-node network with 50% flexible share served as a basis for the simulation. The simulation was carried out on the year 2021 in 8760 time steps, computing deterministic clearing without intraday clearing as a reference. The stochastic clearing was computed with and without intraday corrections prior to balancing.

ECMWF EPS data was used for the day-ahead and intraday forecasts per wind farm and ERA5 reanalysis data served as observation information. The intraday premium factor $\varrho = 0.8$ and extra intraday flexibility $K = 1.2$ were used.

Four indicators were investigated to estimate the significance of the impact of the up-to-down ratio on the day-ahead dispatch and balancing in general. The results are presented in section 4.2.2.

1. Total annually averaged system operating costs $\langle \mathcal{C}_{\text{total}} \rangle_t$
2. Total annual conventional day-ahead dispatch E_s per carrier $s \in \{\text{OCGT}, \text{nuclear}\}$
3. Total annual amount of shedded demand E^{shed}
4. Total annual balancing measures $E^{+/-}$

$$R = \frac{\kappa^+}{\kappa^-} \tag{3.1}$$

κ^+ (%)	κ^- (%)	R (−)
14	3	4.67
13	4	3.25
12	5	2.4
11	6	1.83
10	7	1.43
9	8	1.13
8	9	0.89
7	10	0.7
6	11	0.55
5	12	0.42
4	13	0.31
3	14	0.21

Table 3.11: Variation of cost extras κ^+ and κ^- charged for purchase and repurchase actions by flexible generators. R is the ratio between these cost extras.

3.4.3 Impact of discount from intraday clearing

Including short-term forecasts has a small effect in terms of cost reduction for example when using the stochastic day-ahead dispatch. As the stochastic intraday clearing is anticipating future balancing measures, the premium factor ϱ affects the expected cost decrease with respect to balancing from performing intraday corrections. A sensitivity analysis has been designed which quantifies whether the premium factor provides and incentive to increase intraday corrections and whether this incentive is influenced by the overall level of flexible generation. The discount of intraday clearing cost with respect to balancing is expressed as $1 - \varrho$. This interpretation takes into consideration that flexible generators offer their corrections with a discount in intraday clearing compared to balancing.

The premium factor was varied between 0 and 100% in eleven steps. Deterministic and stochastic clearing were calculated on the five-node network with 30 and 100% flexible share. Balancing measures were calculated with intraday corrections performed beforehand. Analogous to the analysis of the flexible share, simulations have been carried out over 8760 time steps of the year 2021. The cost extras from table 3.3 were used. Day-ahead and intraday forecasts were obtained from the ECMWF EPS and observations taken from the ERA5 reanalysis data set. The premium factor has been rewritten as a discount factor $1-\varrho$. The extra intraday flexibility $K = 1.2$ was used.

Key indicators were employed to estimate the significance of the impact of the premium factor on the intraday corrections and balancing in general. Three indicators were investigated with respect to the premium factor. The results are presented in section 4.2.3.

1. Total annually averaged system operating costs $\langle \mathcal{C}_{\text{total}} \rangle_t$
2. Total annual amount of shedded demand E^{shed}
3. Total annual intraday corrections $E^{+/-,*}$

Chapter 4

Results

4.1 Two-node network

It has been illustrated in literature that stochastic clearing is able to reduce system operating costs on specific case studies. However, so far ensemble forecast data has not been used in this optimization. Integrating ensemble forecasts instead of limited scenarios (e.g. high and low scenario in the work of Morales et al. (2014)). Using ensemble forecasts dissolves the discrete boundaries set by scenarios and provides a range of scenarios that can be investigated.

In the two-nde network, a constant load is installed at two different nodes which has to be met by the conventional generators G1, G2, and G3, as well as the stochastic generator WP. Probabilistic day-ahead and intraday forecasts of the Nordergründe wind farm serve as an input to generator WP. Deterministic and stochastic day-ahead clearing, with and without intraday clearing prior to delivery was performed for the year 2021 in hourly resolution.

This data basis is used to take a first glance on the following question: How does the use of uncertainty information from power forecasts improve the dispatch of generators? First, total costs are studied, then the treatment of a load shedding event is compared between deterministic and stochastic dispatch. In a further step, the effect of integrating short-term forecasts is studied.

4.1.1 Comparison of deterministic and stochastic clearing

4.1.1.1 Total system operating costs

The total system operating cost, also referred to as total operating cost $\mathcal{C}_{\text{total}}$. It has been defined in equation 4.1, as the sum of day-ahead (DA) dispatch $\mathcal{C}_{\text{DA}}$, intraday (ID) correction $\mathcal{C}_{\text{ID}}$, and balancing measure costs $\mathcal{C}_{\text{BM}}$ divided by the total demand per time step. The annually averaged total system operating costs $\langle \mathcal{C}_{\text{total}} \rangle_t$ for deterministic dispatch are 21.470 €/MWh and 21.077 €/MWh for stochastic dispatch.

$$\mathcal{C}_{\text{total}} = \left(\mathcal{C}^{\text{DA}} + \mathcal{C}^{\text{ID}} + \mathcal{C}^{\text{BM}}\right) / \sum_{n,i} D_{n,i,t} \tag{4.1a}$$

$$\langle \mathcal{C}_{\text{total}} \rangle_t = \frac{1}{8760\,\text{h}} \sum_{t=1}^{8760} \mathcal{C}_{\text{total}} \tag{4.1b}$$

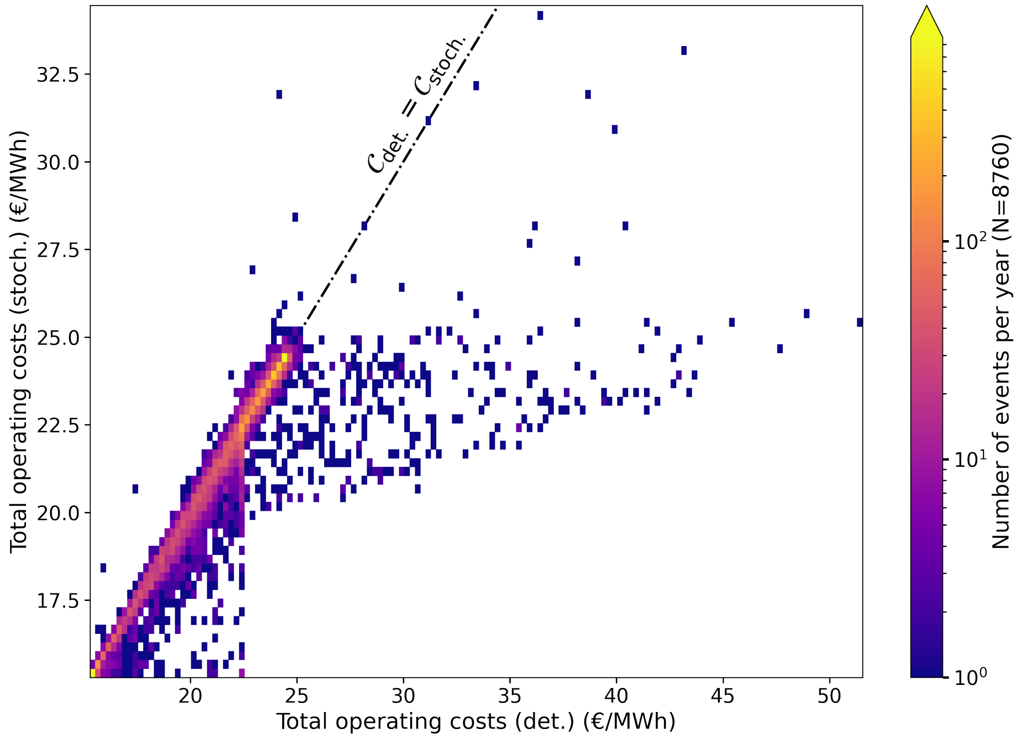

Figure 4.1: A heatmap of total operating costs from day-ahead clearing plus balancing measures for stochastic versus deterministic clearing. Events from 2021 in hourly resolution have been sorted into bins of 0.25 €/MWh.

The difference of total costs is rather small as the majority of costs have been incurred in the day-ahead clearing. Here, the full demand has to be covered by dispatch, which results in a large dispatch of conventional (and stochastic) generation. The costs from day-ahead clearing generally exceed both the costs from intraday clearing and the balancing measures where only forecast updates or errors are balanced out. In the two-node network, if full feed-in is predicted and then no wind blows at the time of delivery, the maximum error to be balanced is 50 MW of wind feed-in or 29.4% of the total demand. This event is expected to be rare, however, deterministic and stochastic dispatch will deal with such a situation differently.

Figure 4.1 shows the hourly total system operating costs of the stochastic clearing plotted against the costs arising from deterministic clearing in 2021. The costs are the result of market clearing without intraday corrections.

The range of hourly total system operating costs in the deterministic clearing reach from 15.29 €/MWh to 55.29 €/MWh. The stochastic clearing can limit extremes in system operating costs to 38.71 €/MWh. In general, low costs correspond to times with high feed-in from wind park WP, high costs are due to high shares of conventional generation. There are many cases where stochastic clearing clearly outperforms deterministic clearing. Take for example an event which costs 48 €/MWh in deterministic clearing, and costs only 25.5 €/MWh in stochastic clearing. Events where stochastic clearing reduces the total costs compared to deterministic clearing are found below the diagonal. A wide spread range of cost improvements is found with stochastic costs between 22 €/MWh and 25 €/MWh where deterministic costs go up to 50 €/MWh. Shedding costs are significantly larger than marginal costs of the flexible generators at 200 €/MWh. Events below the origin line are likely to be caused by load shedding events. The biggest shedding event from deterministic clearing is analyzed in section 4.1.2.

4.1.1.2 Impact of intraday clearing on operating costs

If an intraday clearing stage is added, flexible generators may reduce or increase their dispatch based upon updated forecasts. Two effects are expected. Firstly, total system operating costs are reduced because the flexible generator G1 will perform balancing measures at a reduced cost before delivery. Secondly, corrections to the day-ahead dispatch before delivery will provide additional generation capacity. This capacity is useful if the day-ahead dispatch strongly overestimated the actual feed-in of stochastic generator WP. Hence, intraday clearing is expected to reduce total operating costs. This is shown in figure 4.2.

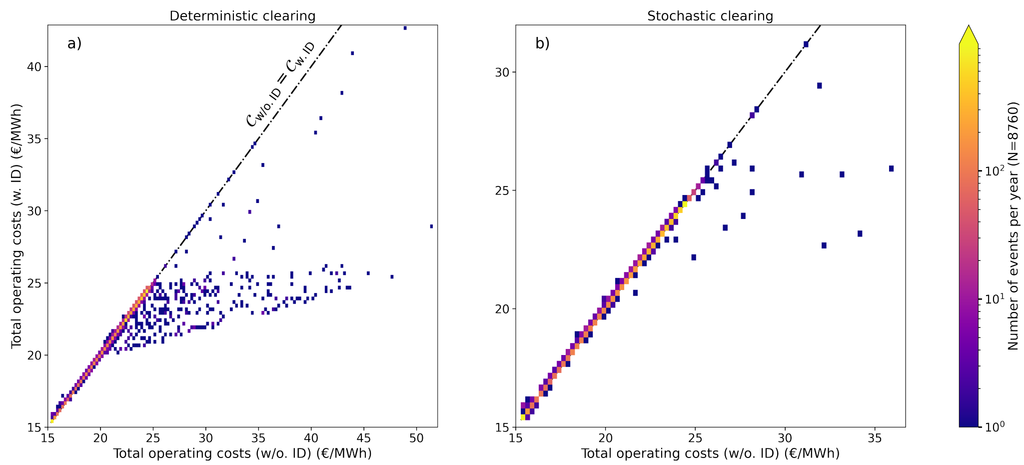

Figure 4.2: The figures shows heatmaps comparing the total operating costs from day-ahead clearing plus balancing measures with optional intraday corrections. The impact of intraday corrections on deterministic (a) and stochastic clearing (b) is compared. Events in hourly resolution from 2021 have been sorted into bins of 0.25 €/MWh.

Total costs including intraday corrections are plotted against those excluding them. Subfigure a) shows deterministic clearing, here most cases have been affected only slightly by intraday clearing and remain close to the origin line as shown by the high density of events here. The main range of costs now lies between 15 €/MWh and 25 €/MWh. Extreme outliers at around 35 €/MWh have been reduced mostly as they are caused by costly load shedding events. Comparing figures 4.1 and 4.2 shows that including intraday corrections affects the same range of outlier events as stochastic clearing does.

The cost reduction expected from clearing generation capacity at a discount is small and lies within 0.25 €/MWh (one bin off to the origin line). Also cost increases occur for all cost levels. Increases of up to 0.5 €/MWh (two bins off the origin line) are for example found at 22 €/MWh but also at lower costs. This shows that the introduction of short-term forecast may affect operating costs also negatively.

Subfigure b) shows stochastic clearing. Here, intraday clearing did also reduce the amount of extreme outliers with costs at 30 €/MWh to 35 €/MWh. Additional capacity for G1 at delivery reduces load shedding. This shows that the provision of additional generation capacity in the day-ahead dispatch is mostly sufficient to reduce very costly load shedding measures. Including intraday clearing further reduces the impact of shedding events which are not covered by the additional flexible generation of G1 planned for in day-ahead clearing. Operating costs are hardly affected in most cases. A slight reduction is gained from clearing at reduced costs (see data just below origin line). However, stochastic operating costs may also be increased which is observed for all cost levels.

In general, it is found that total operating cost averaged for 2021 reduce from 21.470 €/MWh to 21.251 €/MWh in deterministic clearing. Operating cost in stochastic clearing are reduced further from 21.077 €/MWh down to 21.073 €/MWh. Intraday clearing has a positive effect for the reduction of shedding events but may lead to increased costs as well. The effect of cost increase from intraday clearing is studied in more detail in sec. 4.1.3.

4.1.2 Case study: Avoiding shedding by stochastic clearing

It has been indicated in section 4.1.1, that stochastic clearing is able to reduce costs of shedding events. The following section illustrates how stochastic clearing uses uncertainty information to reduce shedding. A time span of three days from the 10th to the 12th April is compared between deterministic and stochastic clearing without intraday corrections. This period features a number of large shedding events including the most severe event on 11th April at 08:00, where the total system cost reaches 55.29 €/MWh.

Figure 4.3 shows the deterministic day-ahead forecast and observation, and the deterministic day-ahead dispatch of generators, as well as the corrections to the dispatch of G1 and load shedding for balancing.

The calm wind on 11th April between 06:00 and 14:00 was not predicted by the deterministic day-ahead forecast which predicted feed-in at nominal power. The maximum error was 50 MW at 08:00 (see figure 4.3a). The observed feed-in was lower than the forecast from 00:00 of 11th April until 10:00 of 12th April.

WP is dispatched up to its forecast level due to zero marginal costs, with G2 and G3 then being dispatched to fill the remaining load (see figure 4.3b). If the wind forecast is low or zero as it occurs on 10th April, G1 is dispatched to cover the remaining 10 MW. On the 11th April, where wind forecast is high, G1 does not have to be dispatched as the predicted wind feed-in is at its nominal capacity. Here, WP covers 50 MW of the electricity demand.

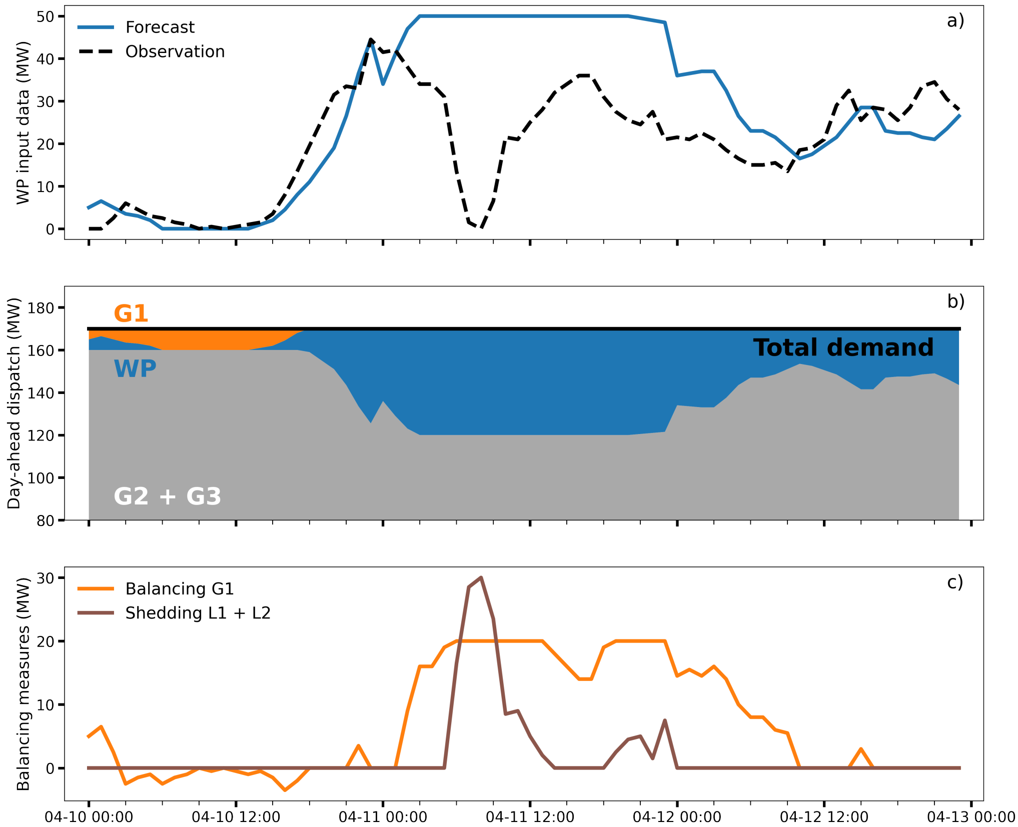

Figure 4.3: Deterministic clearing: An investigation of the system status during a load shedding event on 11th April at 08:00. The forecast and observation data of WP used for day-ahead clearing and balancing (a), resulting day-ahead dispatch of all generators (b), and required balancing measures of G1 and of load shedding L1 and L2 (c).

Minor forecast errors such as on the morning of the 11th April can be balanced easily by ramping up G1 (see figure 4.3c). At 08:00 of the same day, however, no wind feed-in was observed, but 50 MW had been forecasted. 30 MW of load had to be shed as G1 had not been dispatched in day-ahead clearing, therefore it was able to feed-in only up to its ramping limit of 20 MW. The same issue occurred later between 18:00 and 22:00 again as G1 reached its ramping limit.

The load shedding events happened because the day-ahead forecast was taken as granted. Inspecting the same situation in stochastic clearing, the load shedding events could be mostly prevented. This was achieved by taking the probabilistic nature of weather forecasting into consideration when scheduling G1 at the day-ahead clearing stage.

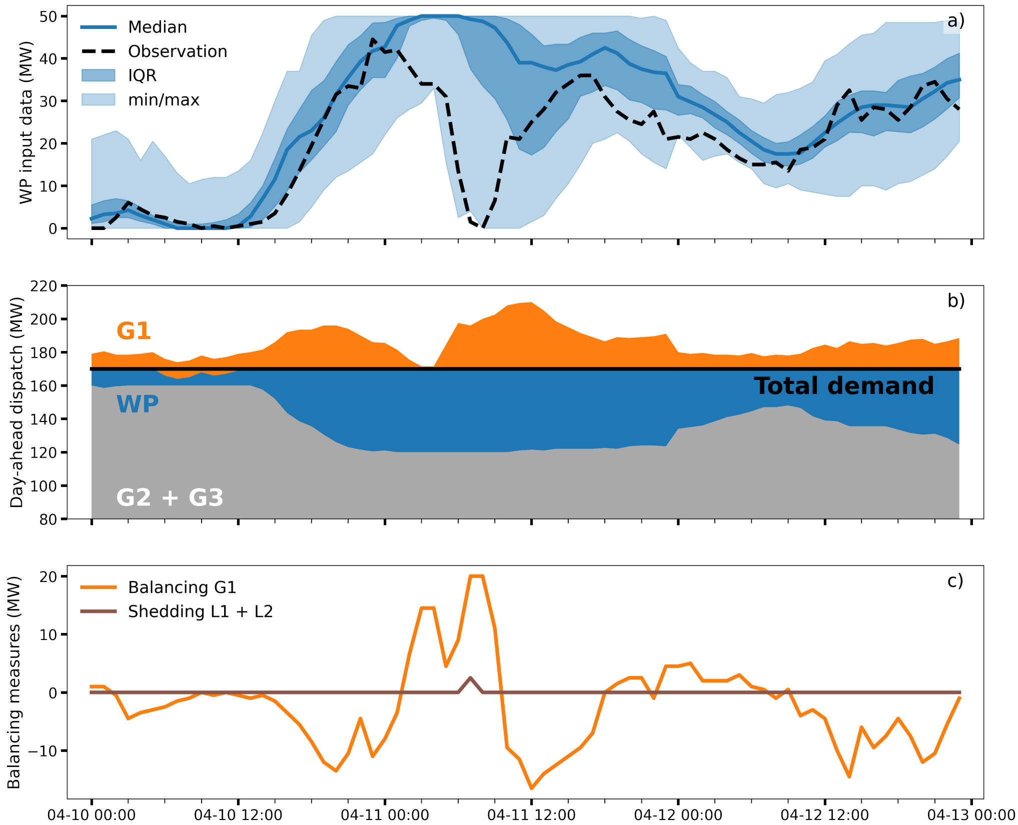

Figure 4.4: Stochastic clearing: An investigation of the system status during a load shedding event on 11th April at 08:00. In the top figure (a), the ensemble forecast instead of the deterministic forecast is shown together with observation data of generator WP (a). The day-ahead dispatch of all generators is shown in the middle (b), and required balancing measures of G1 and loads L1, L2 are shown at the bottom (c).

Figure 4.4a shows that the probabilistic forecast contained information about the strong decrease of wind feed-in during 11th April. The observation lies mostly within or close to the IQR of the ensemble. On 11th April, the forecast ensemble is very narrow at midnight, but then broadens drastically until 06:00. The min/max range spans from 4 MW to 50 MW, and the IQR increases to 16 MW at 08:00. After that, the forecast median decreases to 38 MW, and the IQR broadens further. During this day, the forecast ensemble is very asymmetrical, with most members predicting feed-in close to nominal capacity. From 12th April at 00:00 on, the ensemble becomes symmetrical again. While the IQR and min/max-range are tight at first, they broaden from 12:00 until midnight of that day.

Figure 4.4b shows that the dispatch of G1 considers the information that the forecast is very uncertain. A detailed description of the 10th and 11th April illustrates a linear correlation between the forecast spread and the dispatch of G1. On 10th April, G1 is dispatched up to 10 MW during the entire day. This excess is increased on the afternoon during the ramp up. At 18:00, the forecast spread is 19 MW, resulting in a 27 MW dispatch of G1. At midnight of the 11th April, the forecasts spread is 20 MW and G1 is dispatched up to 25 MW. The spread then reaches its maximum at of 30 MW at 12:00, which resulted in a 40 MW dispatch of G1. As the ensemble spread decreases, the dispatch of G1 decreases to around 10 MW.

Figure 4.4c shows the balancing measures. G1 is reduced for most events to allow the feed-in of WP. This reduction may even lead to an increased share of WP generation compared to the deterministic clearing as less G2 and G3 had been dispatched initially (compare det. and stoch. dispatch on 11th April at midnight). The increase of G1 lead to a vast reduction in load shedding. The sudden drop in WP feed-in on 11th April is mostly balanced by G1 that is ramped up from an already quite large level that was planned at the day-ahead clearing. Only 5 MWh of load had to be shed.

The dispatch of flexible generator G1 in the day-ahead clearing is driven by the forecast feed-in of WP. While also G2 and G3 may potentially be affected, G1 is most important. Its day-ahead dispatch determines the level of forecast errors that can be balanced out at delivery. The time series from above can therefore be abstracted to simple scatter plots of DA dispatch of G1 against some measure of the day-ahead forecast of WP. In the deterministic case, G1 is simply plotted against the deterministic forecast. As WP is always dispatched up to the forecast maximum, G1 only fills up the residual not covered by WP, G2, and G3. In the stochastic clearing, the central tendency of the WP forecast affects the dispatch of G1 less than the spread of its forecast members.

The day-ahead dispatch of G1 is plotted against both forecast median and inter-quartile range (IQR) in figure 4.5. The deterministic dispatch has been added for reference only (see figure 4.5a). It can be seen, that the dispatch of G1 decreases as the forecast of WP increases up to 10 MW, beyond which no dispatch occurs. The stochastic dispatch on the contrary does not correlate linearly with the forecast median but rather suggests a constant dispatch of 10 to 15 MW. As already discussed above on the time series (figure 4.4b), the stochastic day-ahead dispatch of G1 correlates with a measure of the forecast spread. This is shown in figure 4.5b where DA dispatch of G1 is plotted against the inter-quartile range of the DA forecast.

The dispatch of G1 increases linearly with the IQR. A forecast IQR of 0 MW corresponds to a dispatch of 0 MW or 10 MW, depending on the forecast median. The dispatch increases to 22 MW for an IQR of 20 MW. The maximum dispatch of 40 MW may be reached when the IQR is greater than 25 MW. The events are scattered broadly, which means that the dispatch cannot be explained solely by the inter-quartile range. To illustrates what this means, consider an example with a spread below 5 MW where low and high median events are clearly separated. High median events do not require additional flexibility in general. There are however some

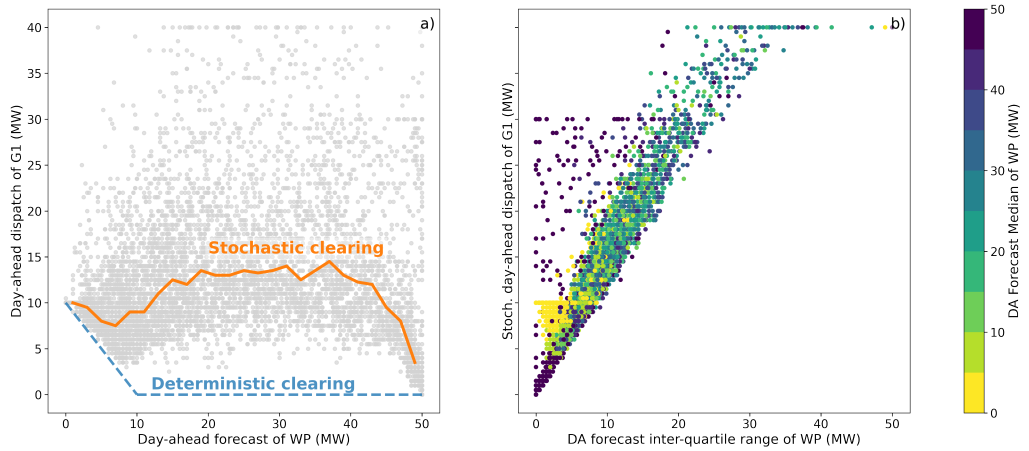

Figure 4.5: The sensitivity of day-ahead dispatch of flexible generator G1 is studied in stochastic clearing. On the right (a), the day-ahead dispatch of G1 is scattered against the ensemble forecast median of WP. To compare with the deterministic dispatch (represented by blue line), the median value of stochastic dispatch was sorted into bins of 2 MW width (shown as orange line). On the left (b), the correlation between stochastic day-ahead dispatch of G1 and the forecasts inter-quartile range is shown. Here, the color scale represents the forecast median.

events with high median where the inter-quartile range may be small or zero but the smallest forecast member is still be a strong outlier. This then results in a day-ahead dispatch of 30 MW. Such an event is for example found in figure 4.4 at 9:00. The median is large, the spread is very small but some members predict zero feed-in. In this case, the observation did then indeed drop to zero.

Therefore, the use of the forecast ensemble for procurement of surplus dispatch or flexible reserve depends on the forecast median. If the median is low to medium, then the inter-quartile range (or the central 50% of members) are mostly sufficient to determine the dispatch. If, however, the forecast median is high but the spread is low, then it is worth taking the full ensemble into account, as the IQR might not contain all valuable information.

4.1.3 Case study: Increase of total cost through intraday clearing

The difference in total operating costs $\mathcal{C}_{\text{w/o. ID}} - \mathcal{C}_{\text{w. ID}}$ of a clearing configuration with and without intraday clearing prior to balancing is compared from hereon. In general, one expects short-term forecasts to predict the stage of delivery better which makes the investigation of events with cost reduction less interesting and the focus is put on increases instead. The cost increase through intraday clearing which was identified in the section above is studied in depth for stochastic clearing as including uncertainty information is expected to remove most events where a poor decision is made by not knowing its impact at delivery (which would be the case in deterministic clearing).

Figure 4.6 shows the time series of cost increase over one year which are then abstracted into an histogram. Small cost increases are measured throughout the year. Strong increases occur more often in winter and spring. In total, 784 events of cost increase have been registered with a mean of 0.076 €/MWh.

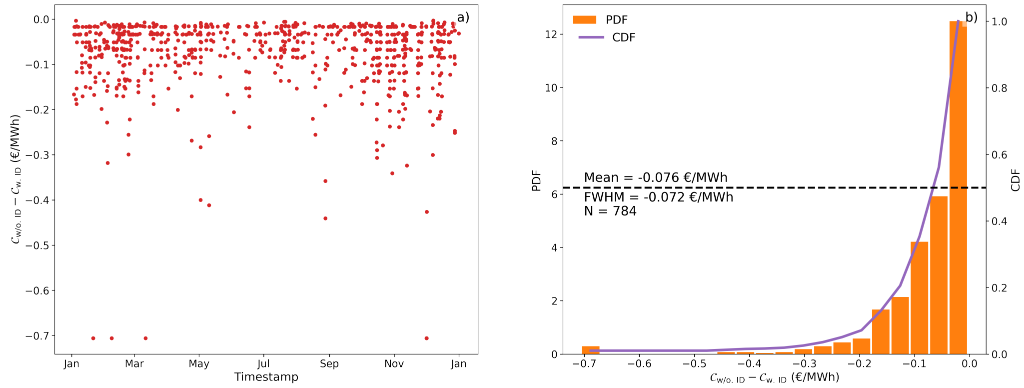

Figure 4.6: Analysis of events with cost deterioration in stochastic clearing with intraday corrections. A time series of the cost difference obtained when subtracting total operating cost with intraday clearing from those without is shown in (a). A histogram of the cost difference is given in (b) with a mean of -0.076 €/MWh.

To illustrate what occurs at events in which operating costs are increased by intraday clearing, events from the 18th to the 20th March are shown together in figure 4.7. Here, medium to strong cost increases are expected from the time series above. Day-ahead and intraday forecast data is shown in subfigure a, the reactions by flexible generator G1 are shown in subfigure b and the difference between total costs without and with intraday clearing is shown in subfigure c.

Three events shall be compared. The first one takes place on the 18th March from 18:00 until 21:00. The second one occurs on the 19th March at 03:00 and the third one is on the same day at 11:00. First, the DA and ID forecasts are compared to the observation, then, balancing and intraday corrections are described, and lastly, the effect on the cost difference is evaluated. Taking a look at figure 4.7a, where the forecasts and observation of WP are displayed, the choice of dates shall be justified briefly. In the first event, the DA forecast predicts the observation well while the ID forecast overestimates the feed-in strongly. The DA forecast median and the observation lie around 10 MW at 18:00 while the ID forecast predicts 24 MW with a small spread. In the second situation, both DA and ID forecast overestimate the wind feed-in. DA median predicts 14 MW, while ID median lies at 19 MW. The observation falls short at 5 MW. The third and last event of interest is an example where the ID forecast performs better at predicting the observation. On the 19th March at 11:00, the DA median lies at 19 MW. The observation however is significantly lower at 2 MW. This decrease has been captured by the ID forecast median with a prediction of 6 MW.

Now, the reaction of G1 to forecast updates and errors in the intraday clearing and balancing in figure 4.7b is studied. First, the balancing measures without prior intraday clearing is described, which is then compared to the impact of intraday corrections onto balancing measures. In the first event, generator G1 is reduced by 11 MW at 18:00, and by 6 MW at 21:00. This strong reduction is likely due to the large dispatch in the day-ahead clearing due to increased forecasts spread. If intraday clearing is performed prior to delivery, then 8 MW are reduced in the ID clearing already, and only 3 MW have to be reduced in balancing. This advantage occurs since the observation lies loser to the ID forecast. At 21:00, 7.5 MW of G1 generation are repurchased

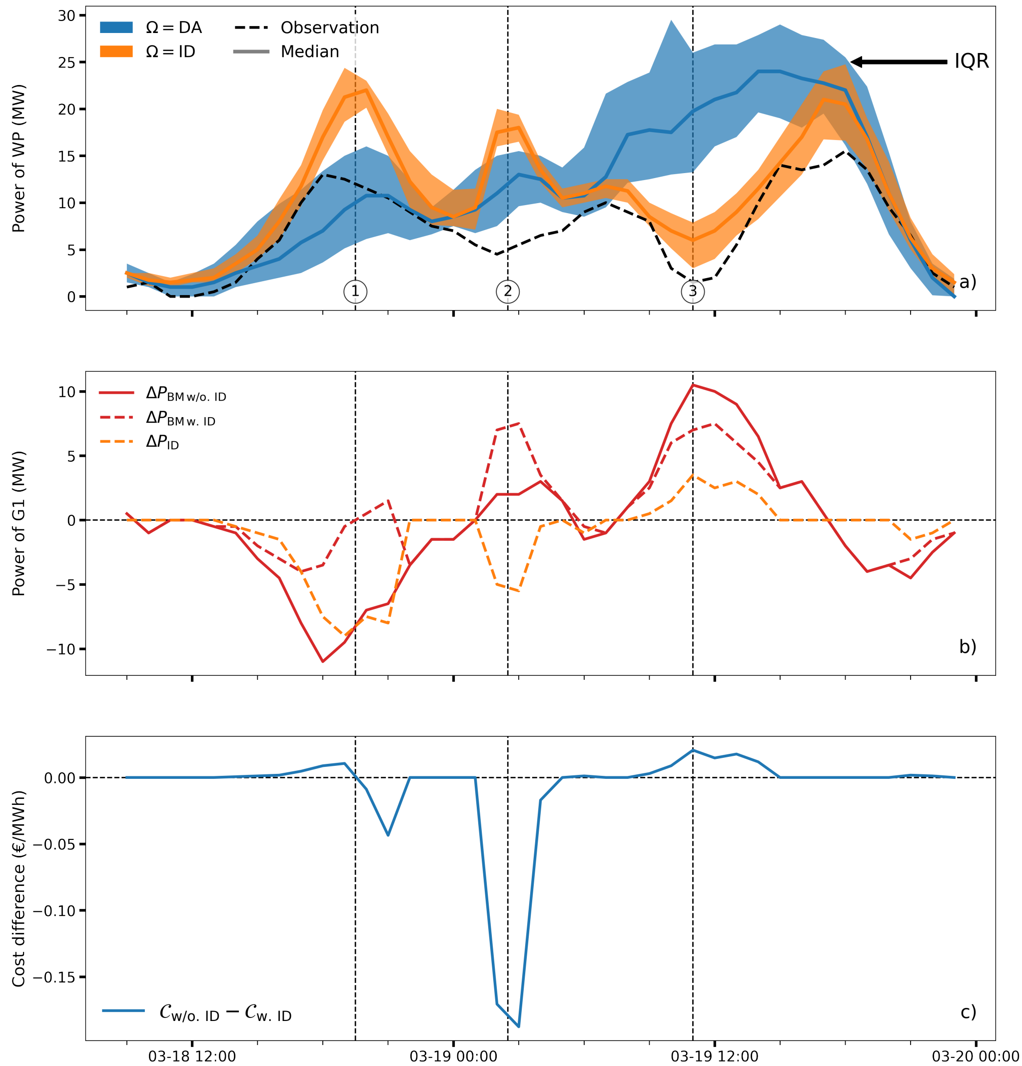

Figure 4.7: This graph shows reactions of G1 in balancing and intraday clearing due to forecast errors. Observed potential wind power feed-in (black line), day-ahead and intraday forecasts are shown in (a). The forecast median and spread are highlighted as well. The reaction of G1 without intraday clearing $\Delta P_{\mathrm{BM\,w/o.\,ID}}$ is compared to intraday corrections ΔP_{ID} and balancing after intraday clearing $\Delta P_{\mathrm{BM\,w.\,ID}}$ (b). The resulting cost difference $C_{\mathrm{w/o.\ ID}} - C_{\mathrm{w.\ ID}}$ is plotted in (c).

in the ID clearing. This repurchase was to large, as the observation was significantly lower and therefore 1.5 MW had to be purchased at balancing. In the second event, the observation turns out too small, and therefore 3 MW have to be purchased in balancing. As the ID forecast over predicted this event, the dispatch of G1 is even reduced by 5 MW. Consequently, the dispatch of G1 had to be increased by 8 MW for balancing. The third event shows a strong over prediction from the DA forecast which leads to a repurchase of 10 MW at the balancing. The mis-prediction could be buffered by the intraday corrections, as 3.5 MW of capacity were already procured in ID clearing, and the remaining 6.5 MW were purchased for balancing.

The impact on costs is shown in figure 4.7c. The first event featured both a slight improvement of costs as well as an increase from intraday corrections. The second event resulted in a strong cost increase due to an adjustment which turned out to be not beneficial to the efficient system operation. The third event experienced only a slight improvement of costs. This shows that the total system costs are much more sensitive to false corrections than corrections which are system-friendly. This sensitivity is due to the large difference between cost extras for purchase κ^+ and repurchase κ^-. Furthermore, the analysis showed that the impact of intraday clearing on total system costs is not bound to the magnitude of the forecast error. The additional ID forecast overestimation relative to the DA forecast was only 5 MW on the 19th March at 03:00, compared to the ID forecast improvement at 11:00 of 14 MW, the former lead to a stronger repurchase of capacity than the purchase of the latter. A smaller forecast update therefore lead to a much bigger cost deterioration.

4.1.4 Conclusion

It was shown that stochastic dispatch reduces annually averaged total system operating costs by reducing the amount of load shedding. The total system operating costs of stochastic clearing are 21.077 €/MWh compared to costs from deterministic clearing at 21.470 €/MWh. Additional flexible generation is procured in the day-ahead clearing by including uncertainty information into the optimization process.

The day-ahead dispatch of flexible generator G1 in stochastic clearing does not correlate linearly with the central tendency of the probabilistic forecast. A strong correlation between forecast spread and the dispatch of G1 was discussed. It was also discussed that strongly asymmetric ensemble forecasts lead to deviations from the linear correlation.

In addition to that, the impact of intraday clearing was investigated. Intraday clearing reduces annually averaged total system operating costs too. Deterministic intraday clearing reduces costs from 21.470 to 21.251 €/MWh. As stochastic clearing has already reduced most shedding events in comparison, the extra impact of intraday clearing is small, decreasing the total system operating costs from 21.077 to 21.073 €/MWh.

Scatter plots revealed events in which operating costs are increased by intraday clearing prior to balancing. It was found that total operating costs are more sensitive if the short-term forecast deteriorates with respect to the day-ahead forecast than if it improves. An increase occurred in 784 hours of the year by an average of 0.076 €/MWh. A forecast deterioration which resulted in a cost increase of 0.17 €/MWh was compared to an event with a forecast improvement leading to cost reductions by 0.03 €/MWh. This discrepancy between cost increases due to forecast improvement, and cost increases due to forecast deteriorations, is large. It was explained considering the cost extras for upward and downward corrections in intraday clearing and balancing.

4.2 Five-node network

A short introduction to the five-node network and previous work shall explain the choice of studies which have been performed on the network. The network has been designed to investigate the impact of probabilistic forecasts on a more realistic network. Realistic in a sense, that there is more than one stochastic generator, the nodal load is not constant and the network is not able to bear the full feed-in from wind farms. A similar study has already been carried out in a Bachelor thesis (Buller, 2023) parallel to my work where the five-node network had been investigated in which the conventional generation was fully covered by open-cycle gas turbines (OCGT). The influence of the distribution of flexible generation on load shedding, curtailment and total system costs. Furthermore, the impact of increased transmission link capacities was evaluated based on the same parameters. The biggest shedding event has been tracked down to a transmission network congestion. Increasing the transmission capacity lead to a decrease of shedding, however, load shedding was increased. This study is very interesting but also restricted as it assumed the best possible network layout in terms of flexibility as all generators may be adjusted during the balancing at delivery. In this case, the difference in total system operating costs, load shedding and curtailment was small. Adding intraday clearing to the processing chain did not have a strong effect (see table 4.1). While this is an interesting result in and of itself, and one could go on and study more discrete weather scenarios by looking at the temporal variation, my interest was drawn to the bigger question of how to measure the advantage of utilizing uncertainty information in power systems management. If the system is fully flexible, this advantage is rather small.

Clearing sequence		$\langle \mathcal{C}_{\text{total}} \rangle_t$ (€/MWh)	E^{shed} (MWh)	E^{curt} (MWh)
deterministic	w/o. ID	2.555	159 627	18 447 673
	w. ID	2.452	46 601	18 409 869
stochastic	w/o. ID	2.379	1 448	18 402 399
	w. ID	2.378	398	18 400 934

Table 4.1: Key indicators from the five-node network with conventional generation fully covered by open-cycle gas turbines (OCGT).

Therefore, I investigated the sensitivity of several key indicators to the some input parameters of the model. This is an important study as it showcases how uncertainty information may gain or loose value with respect to deterministic forecasts and dispatch. The analysis of key indicators will also help to identify events where the use of uncertainty information is especially critical. It also provides a more general grasp on quantities in the model such as day-ahead clearing, intraday clearing and balancing measure volumes.

Throughout the sensitivity study, the reader will encounter two reference units. These are used to make abstract amounts of energy more tangible. The total annual demand is the total amount of energy which has to be cleared in order to ensure the nodal balancing constraint of the optimization. The total annual observed wind power potential is a measure for how much wind energy is available throughout the year in the system. Both parameters are given in table 4.2.

Reference	Formula	Value
Total annual demand	$\sum_{n,i,t} D_{n,i,t}$	139 583 415 MWh
Total annual observed wind power potential	$\sum_{n,s,t} \tilde{O}_{n,s,t} \bar{G}_{n,s}$, $s \in \{\text{onshore, offshore}\}$	81 001 946 MWh

Table 4.2: Constants of the five-node network used throughout section 4.2.

4.2.1 Sensitivity to installed flexible generation capacity

4.2.1.1 Total system operating costs

Figure 4.8 shows the annual average of total costs $\langle \mathcal{C}_{\text{total}} \rangle_t$ (see equation 4.1) resulting from deterministic and stochastic day-ahead (DA) dispatch including optional intraday (ID) correction costs and resulting balancing costs. The costs are plotted against the share of flexible generator capacity installed relative to the total installed capacity of conventional generators (referred to as *flexible* or *OCGT* share). The total conventional generation capacity accounts for 46.8% of the conventional and stochastic capacity combined (see table 3.7). Keep this in mind, when interpreting the flexible share. A share of 50% corresponds to 23.4% of installed OCGT generation capacity.

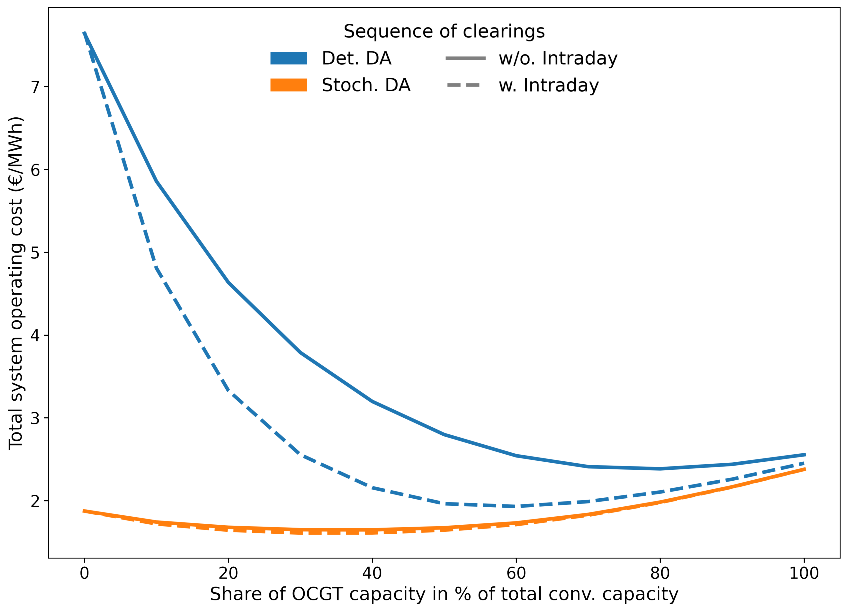

Figure 4.8: The total system operating costs have been plotted against the share of installed flexible OCGT generation capacity for deterministic (shown in blue) and stochastic (shown in orange) clearing with (dashed line) and without (solid line) intraday corrections.

Deterministic clearing is overall more expensive than stochastic clearing. If conventional capacity is fully covered by inflexible nuclear power plants (i.e. 0% OCGT share), total costs from deterministic clearing are at 7.644 €/MWh whilst including uncertainty into the planning leads to total costs of 1.875 €/MWh.

The impact of including uncertainty into scheduling decreases with an increasing share of flexible generators. At 30% OCGT share, total costs without intraday clearing under stochastic day-ahead scheduling reduce to a minimum of 1.649 €/MWh, with deterministic clearing still at more than double the costs with 3.789 €/MWh.

The total cost for deterministic clearing decrease to a minimum of 2.385 €/MWh at 80% OCGT share. Increasing the OCGT share further leads to an increase in total costs as OCGT is more expensive than nuclear.

The same trend is found for the stochastic clearing. At 100% OCGT share, stochastic total cost are highest at 2.379 €/MWh only slightly cheaper than deterministic clearing without ID at 2.555 €/MWh.

The total operating costs without intraday corrections depend on the share of OCGT capacity relative to the total conventional capacity installed. At least two effects have to counteract each other which then leads to a cost minimum for both deterministic and stochastic clearing. An increase in operating costs is to be expected from increasing shares of OCGT capacity. This effect is investigated in section 4.2.1.2. The strong decrease in deterministic total costs is likely due to expensive load shedding which is further investigated in section 4.2.1.3.

Reduction of operating costs through intraday clearing Intraday clearing reduces operating costs for both deterministic and stochastic clearing.

The reductions in operating costs from deterministic clearing are always higher than those of stochastic clearing. At 10% OCGT share, the deterministic savings from ID corrections are 1.049 €/MWh, the stochastic savings are only 0.022 €/MWh.

The maximum savings of both deterministic and stochastic clearing are found at 30% OCGT share with 1.234 €/MWh and 0.040 €/MWh respectively. The savings then reduce again to minor influence at 100% OCGT share, where deterministic clearing saves 0.612 €/MWh and stochastic clearing saves 0.020 €/MWh with ID corrections.

The operating costs of the stochastic clearing are already lower. As explained in section 4.1.2, this is due to the additional flexibility in the day-ahead clearing. To understand why the impact of intraday clearing is reduced, a moment with large spread at the day-ahead forecast shall be considered as an example. It has been shown on a simple network, that the spread results in a higher procurement of OCGT (see section 4.1.2) to reduce anticipated balancing measures. In the intraday clearing, a more precise but reduced forecast is provided. Since flexibility had already been dispatched in the day-ahead clearing, short-term changes are no longer necessary or only to a limited extent.

Analogously, one can explain why costs in deterministic clearing are so strongly influenced by intraday clearing. The lack of flexibility in the day-ahead dispatch can be corrected based on forecast updates.

4.2.1.2 Conventional annual day-ahead dispatch

Figure 4.9 shows the total annual conventional day-ahead dispatch (see equation 4.2). The shares stemming from nuclear or OCGT generation are stacked. The grey line and light colored areas correspond to the stochastic clearing, the black line and darker shaded areas are the deterministic results plotted on top.

$$E_s = \sum_{t=1}^{8760} \sum_{n} G_{n,s,t} \tag{4.2}$$

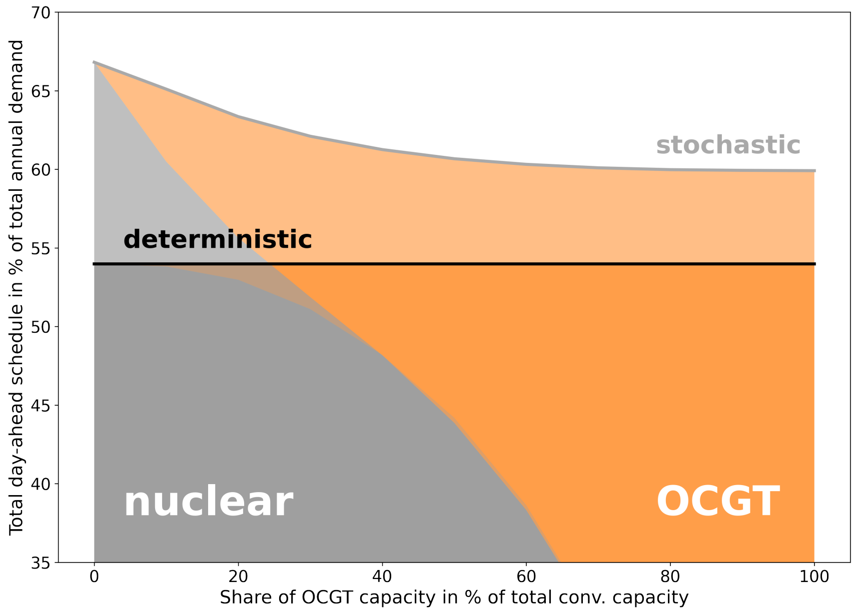

Figure 4.9: The total day-ahead dispatch of conventional generators has been plotted against the share of installed flexible OCGT generation capacity. The total stochastic day-ahead dispatch is represented by the grey line, the deterministic equivalent is given by the black line. Inflexible nuclear dispatch (grey) and flexible OCGT dispatch (orange) are stacked on top of each other. The y-axis starts at 35% to highlight differences in dispatch at low shares of OCGT.

The total deterministic day-ahead generation remains unaffected by the share of flexible generators. While the capacity dispatched by the deterministic DA clearing covers the demand exactly, the stochastic day-ahead clearing plans for a capacity surplus of both nuclear and OCGT generators for all shares of flexible generators. This can be viewed as a reserve to prevent balancing as discussed in section 4.1.2.

For a share of 0% OCGT, the deterministic clearing covers 54.0% of the demand with conventional generators. The stochastic clearing plans for 66.8% of conventional generators, i.e. an extra of 12.8%. This additional capacity is reduced with increasing shares of OCGT. At 30% share of OCGT, stochastic clearing plans for 8.1% more, at 100%, 5.9% of day-ahead capacity are added.

The scheduling of reserves depends on the share of flexibility. For less than 30% of OCGT share, not only additional OCGT generation is planned but also additional nuclear generation. At 0% OCGT share, 12.8% more nuclear generation is dispatched compared to only 5.9% more for 100% OCGT share. This dependency can be easily understood when considering a wind power forecast with a high spread. If the spread is large, events with small wind feed-in are likely. Since short-term flexibility is low due to the lack of OCGTs, shedding of demand remains as the only balancing measure available. To avoid these very costly shedding events (see tab. 3.6), additional nuclear generation is planned to replace the wind power. Nuclear generation serves as a sort of security against unreliable wind power supply.

Two questions arise from this diagram. Under which situations is additional OCGT capacity planned? How does OCGT replace the inflexible nuclear generation when the share of OCGTs is increased? These questions are addressed in section 4.2.2. Here, the cost extra charged for upward and downward corrections in balancing with respect to the day-ahead clearing are varied. The variation leads to different expected balancing costs which impact the day-ahead dispatch.

4.2.1.3 Total annual load shedding

Figure 4.10 shows the total annual amount of load shedding (see equation 4.3) relative to the total annual demand against the share of OCGT generator capacity installed. Deterministic and stochastic clearing with and without intraday corrections are compared. Load shedding occurs if the predicted feed-in from wind farms is higher than the observed feed-in and the resulting mismatch cannot be balanced out by flexible conventional generators. Shedding remains as the only option to keep nodal balance.

$$E^{\text{shed}} = \sum_{t=1}^{8760} \sum_{n,i} S_{n,i,t} \tag{4.3}$$

An analysis of the strongest load shedding events on the fully flexible five-node network (i.e. 100% flexible share) (Buller, 2023) showed that shedding occurs if the error between day-ahead forecast and observation for a wind farm is so large that it cannot be balanced out by flexible generators. If additionally network constraints limit the delivery of power from other buses, shedding of load is the only available option to ensure nodal balancing. Load shedding is much more likely in deterministic dispatch than stochastic because the deterministic forecast solely predicts wind feed-in. If the forecast is high enough, no flexible generators are included in the dispatch and thus strong forecast errors cannot be balanced out.

Load shedding is highest if no flexible generators are available. Any underproduction has to be shed. Deterministic dispatch leads to total load shedding of 4.1% whilst stochastic dispatch leads to only 0.1% shedding of the total annual demand.

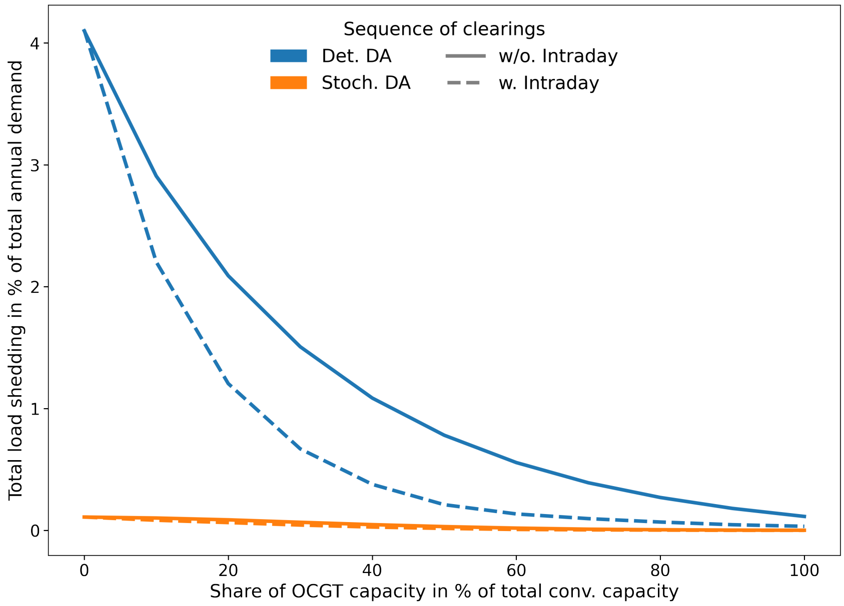

Figure 4.10: The total load shedding relative to the total annual demand is plotted against the share of installed flexible OCGT generation capacity. The deterministic clearing is shown in blue and the stochastic one in orange. A clearing configuration with intraday corrections prior to balancing is represented by a dashed line.

At 30% OCGT share, total annual load shedding from deterministic dispatch has reduced down to less than half at 1.5% with shedding from stochastic dispatch reduced to 0.06%.

Shedding under both deterministic and stochastic dispatch reach a minimum if the conventional power generation capacity is fully covered by OCGTs. Shedding from deterministic dispatch reduces to 0.11% and from stochastic dispatch to 0.001% of the total annual demand.

If flexible generation is not sufficient, shedding from deterministic clearing is large and is always outperformed by stochastic clearing. Through integration of uncertainty into day-ahead dispatch, we find that a reserve between 6 and 13% of conventional generation annually (see section 4.2.1.2) is sufficient to reduce expensive shedding measures.

Reduction of load shedding through intraday clearing The cost reduction in stochastic clearing can be explained mainly by preventing load shedding, as well as by the discounted repurchases of excess OCGT capacity. In deterministic clearing, additional flexible generation prevents load shedding (see figure 4.10).

At 10% OCGT share, deterministic intraday corrections reduce the total shedded energy by 0.7% of the total annual demand. At 30% the reduction is maximum at a difference of 0.84%. Above 60%, deterministic intraday corrections have a smaller effect as the further reduction of load shedding is below 0.1% of the total annual demand. This shows that there is already a sufficient amount of flexible generator capacity installed to cope with a wide range of larger forecast errors by ramping up.

The total load shedding in stochastic clearing is already comparatively low (smaller than 0.1%). The maximum reduction from intraday corrections of load shedding occurs at 30% OCGT share, where an additional 0.02% of the total annual demand are shed less. It is found that above 60% OCGT share, the deterministic dispatch with ID corrections perform similar to stochastic dispatch with (and without) ID corrections. Deterministic load shedding after intraday corrections is 0.03%, and 0.001% (with ID 0.0003%) from stochastic clearing.

Total costs versus costs of shedded load If the shedding costs are excluded from the total system operation costs by omitting the shedding term from $\mathcal{C}^{\mathrm{BM}}$ (see equation 2.3), deterministic and stochastic total system operating costs are much more alike (see figure 4.11).

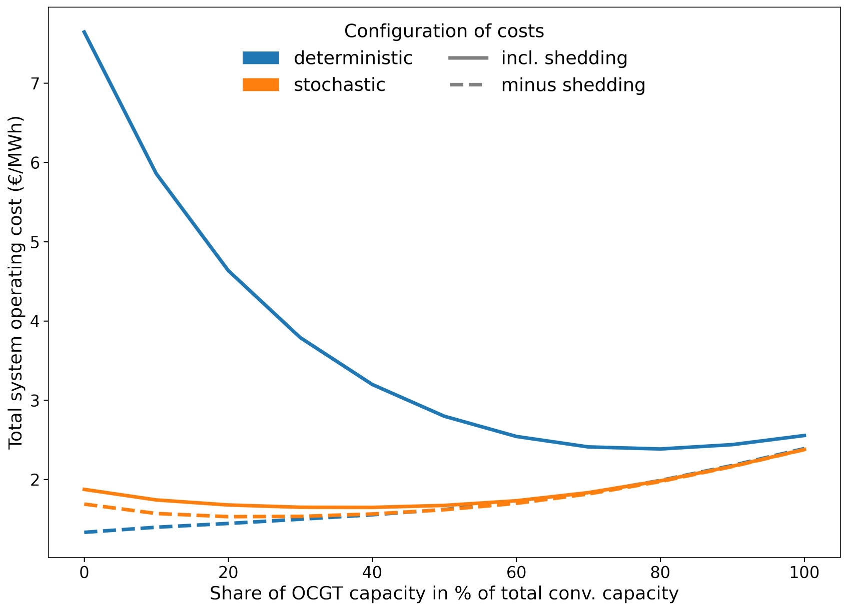

Figure 4.11: Total system operating costs minus total shedding costs for deterministic and stochastic clearing without intraday corrections.

Subtracting shedding costs from the total operating costs, shows that shedding was the dominant driver of deterministic system costs. In addition to that, stochastic dispatch is more expensive than deterministic, if shedding is excluded and the OCGT share is below 50%. This is clear because the dispatch of conventional generators is increased for stochastic clearing when it prevents load shedding. A more precise comparison of total costs excluding shedding would have only compared events where no load shedding takes place in deterministic clearing and averaged over the costs of those events in deterministic and stochastic clearing. At 100% flexible share, stochastic clearing is on average 0.0128 €/MWh less expensive than deterministic clearing. This advantage comes from the procurement of OCGT at reduced costs already in the day-ahead clearing. The overall advantage from procuring flexibility early is small but has the advantage of preventing load shedding.

As load shedding determines the price dominantly, it has to be made clear, that modeling of load shedding or loss of load should not be considered unrealistic and thus the advantage of stochastic clearing is not hypothetical. In reality, demand-supply mismatch does not necessarily correspond to expensive black-out events. In these periods storage is activated or imports from neighboring network regions are necessary (ENTSO-E, 2022). Both processes are not being modeled directly but are found as load shedding events in this work. The stochastic clearing shows that shedding events can be reduced by knowledge of forecast uncertainty.

Compared to national loss-of-load expectation (LOLE) standards which lie between 3 and 8 hours/year (ENTSO-E, 2022) the loss of load duration (LLD) is serious for both clearing methods but most notably in the deterministic clearing. Here, it reduces from 6750 h at 0% down to 289 h at 100% OCGT share. It is not clear whether our results are acceptable within the standards of European transmission grid operators. A quick excursion into the European Resource Adequacy Assessment (ERAA) shall therefore provide a reference. ERAA is a yearly scenario-based outlook on the quality of supply in the pan-European transmission grid. Results include the scarcity of supply assessment which is calculated per European bidding zone.

Scarcity is defined as the energy not served (ENS) which is the sum of load, generation, imports and exports aggregated in a bidding zone. LLD and subsequently LOLE are then defined upon hours with non-zero ENS (ENTSO-E, 2022).

The ERAA studies simulate a highly detailed, interconnected European market with system flexibility provided by various processes including energy storage and cross-border exchange. Since we do not model these two options at the moment, a direct comparison of national LOLE standards and our results should not be drawn. It is to be expected that mismatches in our system are balanced out by both pumped hydro storage and imports from other grid regions.

4.2.1.4 Annual curtailment of wind power

The extra procurement of conventional capacity from stochastic day-ahead dispatch has been discussed as the reason for reduced load shedding in section 4.2.1.3. The curtailment of a wind farm $G^{\text{curtailed}}_{n,s,t}$ measures the difference between potential maximum wind power feed-in $\tilde{O}_{n,s,t}$ and the actual delivered wind power $G^{\text{delivered}}_{n,s,t}$. The delivery is the sum of day-ahead dispatch, intraday corrections and balancing measures (see equation 4.4).

$$
\begin{aligned}
G^{\text{curtailed}}_{n,s,t} &= \bar{G}_{n,s}\left[\tilde{O}_{n,s,t} - \left(G_{n,s,t} + G^{+}_{n,s,t} + G^{-}_{n,s,t} + G^{+,*}_{n,s,t} + G^{-,*}_{n,s,t}\right)\right] \\
&= \bar{G}_{n,s}\left[\tilde{O}_{n,s,t} - G^{\text{delivered}}_{n,s,t}\right] \qquad (4.4)
\end{aligned}
$$

$$
E^{\text{curtailed}} = \sum_{t=1}^{8760}\sum_{n,s} G^{\text{curtailed}}_{n,s,t} \qquad (4.5)
$$

In figure 4.12 the total annual curtailment (see equation 4.5) relative to the total annual potential wind power feed-in is plotted against the OCGT share.

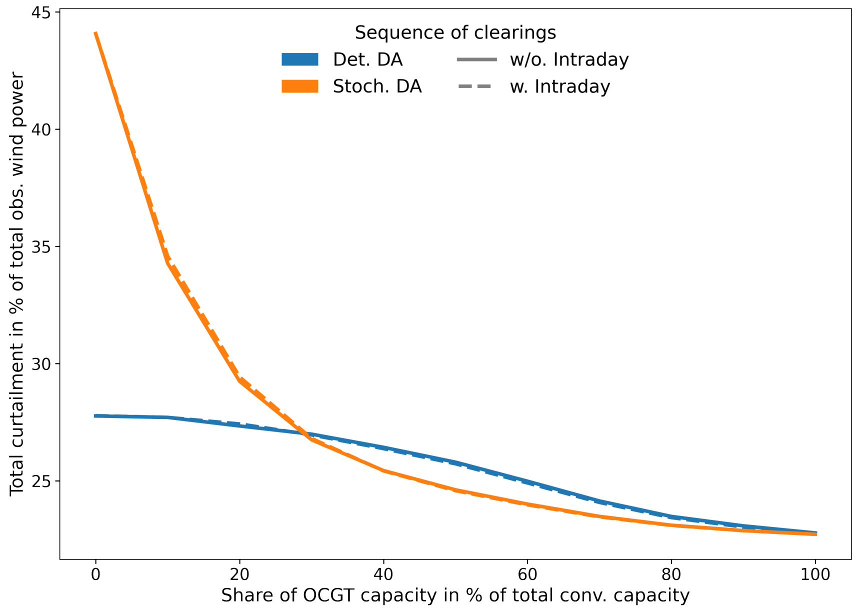

Figure 4.12: The total annual curtailment relative to the total observed wind power is plotted against the share of flexible generators. The deterministic (blue) and stochastic clearing methods are compared with (dashed line) and without (solid line) intraday corrections.

For OCGT shares between 0% and 20%, deterministic clearing outperforms the stochastic clearing by curtailing up to 16.3% less per year. This is due to the procurement of additional inflexible capacity in the stochastic clearing. If wind power exceeds the expected, dispatched generation, it cannot be used to replace conventional generation but has to be curtailed. Here we see, that avoiding load shedding comes at the cost of reduced wind feed-in cost if system flexibility is low.

For a network with shares of flexible generators between 40% and 90%, stochastic clearing performs better than deterministic. Here, stochastic clearing prevents up to 1.2% of curtailment compared to deterministic clearing.

While the curtailed wind energy depends on the share of flexible generators, there is a residual curtailment of 22.7% in both clearing methods at 100% OCGT share.

This residual curtailment is likely due to network congestion. The five-node network has been designed to not be able to transmit the full feed-in of wind farms to the demand hubs. A simple example is the bus *Buettel*, with 2.85 GW of onwind and 4.28 GW of offwind generators installed (see table 3.7). Beyond a predicted capacity factor of 50%, wind power has to be curtailed as the link *Buettel* $\leftrightarrow$ *HH* can only transmit 3.57 GW (see table 3.9). Significant capacity is also installed at the bus *Ems* (9.7 GW), however, only 62% of that can be transmitted to *Ruhr*. Power could also be transmitted to *HH*, but this is likely to be already saturated by the feed-in from *Buettel*. Bus *WHV* is very poorly connected, and thus, both onwind and offwind generators will be curtailed in many events. Stochastic clearing may improve on the curtailment by dispatching higher amounts of OCGT generators when the forecast median is medium to low but the spread is also large, meaning that high feed-in is still likely. Deterministic dispatch might cover similar scenarios with more inflexible generators which cannot be ramped down to make room for wind feed-in.

To put the amount of curtailed generation into perspective, it can be compared to load shedding. The maximum annual amount of load shedding from deterministic clearing is 4% of the total annual electricity demand, the maximum amount of curtailment is 27.8% of potential annual wind feed-in or 16.1% of the total annual electricity demand. Keeping in mind, that storage utilization is not lossless and charge and discharge periods (i.e. curtailment and shedding periods) should be temporarily close (Denholm & Mai, 2019), the amount of curtailed generation still seems sufficient to avoid large amounts load shedding.

Effect of intraday clearing on curtailment Curtailment remains largely unaffected by ID corrections in both deterministic and stochastic clearing as figure 4.12 illustrates well. For small OCGT shares, curtailment is even increased by about 0.1% of the total wind feed-in potential through intraday clearing. An increase in curtailment occurs if generation at a site or in the system is inflexible in general. If wind feed-in is increased and conventional generation cannot be reduced, curtailment has to occur.

For medium to high OCGT shares (larger than 30%), curtailment is reduced by ID clearing. The maximum reduction is measured at 60% OCGT share, with 0.07% being reduced in deterministic and 0.03% of potential wind feed-in in stochastic clearing. A decrease in curtailment is due to additional system flexibility which allows to balance down conventional generation in case of additional wind feed-in.

It is remarkable how small the effect of intraday clearing on curtailment is. Intraday clearing is an early option for adjustments, acting like a balancing in advance. While ID clearing is subject to reduced costs, an advantage of corrections to the dispatch is only gained if the additional capacity in upward and downward corrections (defined as factor K in equations 2.9h, 2.9i) can be utilized. The possibility to do so depends on the share of conventional generation or forecasted wind power in the system. Low conventional feed-in found under high wind penetration can be corrected equally during both intraday clearing or balancing. Increased balancing under low forecasted wind feed-in occurs only in strong ramping events which are expected to be rare.

4.2.1.5 Total annual intraday corrections

$$E^{+/-,*} = \sum_{t=1}^{8760} \sum_{n,s} G_{n,s,t}^{+/-,*} \tag{4.6}$$

Figure 4.13 shows the usage of intraday clearing, which is measured as the total annual amount of intraday corrections (see equation 4.6) divided by the system's annual electricity demand against the OCGT share. The amount of additional generation procured in deterministic clearing increases with the installed flexible generation and approaches an asymptotic threshold of 3.3% of the total annual demand. The purchase of extra OCGT capacity in stochastic clearing

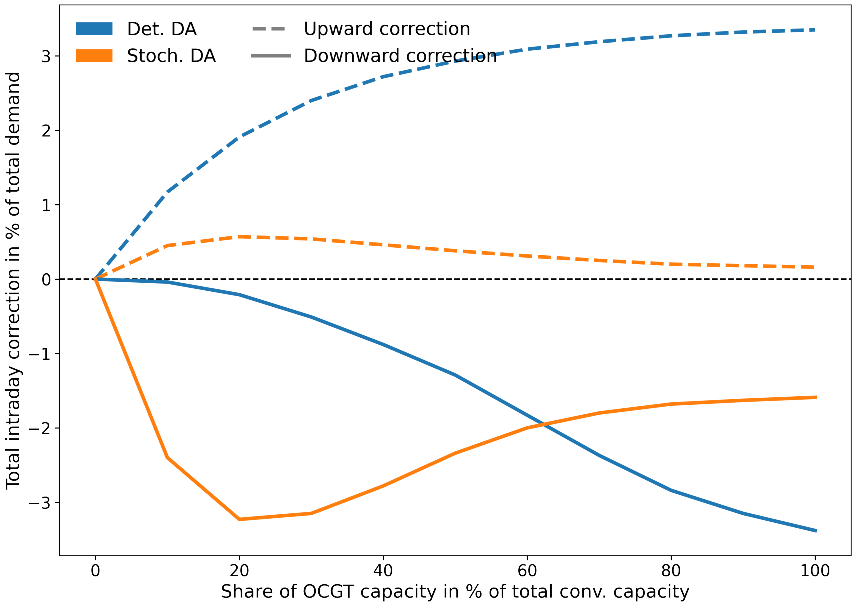

Figure 4.13: Sensitivity study of total annual intraday corrections against the share of OCGT capacity installed. Corrections based on a deterministic day-ahead and intraday implementation are marked blue, stochastic data is marked orange.

attains a maximum of 0.6% at 20% to 30% OCGT share and subsequently declines to 0.1% asymptotically.

Similarly, repurchase or reduction in generation in deterministic clearing rises with installed flexible capacity as well. The increase starts slowly and has the steepest slope at about 60% OCGT share. For larger OCGT shares, the amount of reduction rises further but at a reduced rate reaching a maximum amount of 3.4%. Intraday downward corrections in stochastic clearing reach a maximum of 3.2% when the OCGT share lies between 20% and 30%. The downward corrections decrease slowly, reaching a minimum at 1.6%.

When the share of installed flexible generation capacity increases, the intraday purchases do not increase linearly in deterministic clearing. Consider that the increase for low shares of OCGT corresponds to cases where the small amount of OCGT capacity is sufficient to balance out small forecast errors. Larger forecast errors cannot be addressed due to limited ramping capacities. However, if the OCGT share is increased, this ramping capacity increases as well and thus events with large forecast errors can be balanced out. Extreme forecast errors occur less frequently, hence adding more OCGT capacity opens up fewer additional events for balancing. Therefore, the amount of upward corrections reaches a maximum asymptotically.

In stochastic clearing, the intraday upward corrections reach a maximum at 20% to 30% share of installed OCGT capacity and then decrease again. As it coincides with the strongest reduction of load shedding through intraday clearing, I want to explore a possible reason. Firstly, the day-ahead dispatch anticipates forecast errors and therefore, the amount of upward corrections is smaller than in deterministic clearing. The maximum of intraday corrections is not simple to grasp. On way to explain an extremum is to discuss two processes which counter-effect each other. In the case of intraday upward correction, the flexible stochastic day-ahead dispatch increases with OCGT share. This dispatch is designed to cover for forecast errors. The increase in installed flexible generators also increases the available ramping power (20% of nominal capacity). At 30% OCGT share, the day-ahead dispatch may not be large enough but intraday clearing already reaches a wide range of forecast errors and therefore load shedding may be reduced. Increased dispatch at larger OCGT shares then reduces the requirement for large short-term corrections. The stochastic formulation of the intraday clearing may also reduce the amount of purchase which are expected to increase expected balancing costs.

In deterministic clearing, repurchase is low at first because day-ahead dispatch of OCGTs is small (see figure 4.9) and therefore events with underestimation of wind power, and thus too high OCGT generation, are rare. As dispatch of OCGT increases, the occurrence of such events rises too.

The amount of repurchases increases strongly with OCGT share in stochastic clearing. This shows that a high amount of flexibility has been procured in the day-ahead clearing. Many moments, in which forecast errors were anticipated, have an increased intraday forecast and thus flexible generation is repurchased. The amount of repurchases might be driven by the additional extra flexibility of nuclear and OCGT for low OCGT shares as shown above in figure 4.9.

4.2.1.6 Conclusion

The first sensitivity analysis focused on the influence of the share of flexible generators in the total generation capacity. One reason for the study was to find out how the utilization of short-term forecasts changes with the flexible share. Deterministic and stochastic clearing were analyzed separately, always comparing balancing with and without prior intraday clearing.

Deterministic day-ahead clearing has an increased load shedding completely independent of the flexible share. The highest shedding is 4% of the total annual demand (0% flexible share), the lowest amount was measured at 0.1% (100% flexible share). Stochastic day-ahead clearing reduces the load shedding to 0.1% (0% flexible share) and reduces this further to 0.001% of the total annual demand at 100% flexible share.

If intraday clearing is included in the sequence of clearings, shedding in deterministic clearing can be reduced by up to 0.84% of the total annual demand (from 1.5% load shedding at 30% flexible share). With 100% flexible share, the total amount of shedding can be reduced to less than 0.1% of the total annual demand, making it as efficient as stochastic clearing. In stochastic clearing, the introduction of intraday clearing leads to a small reduction in the remaining shedding. The largest reduction occurs at 30%, where 0.02% of the total annual demand was shedded less. The total amount of shedding in the five-node network was compared to network adequacy assessments methods. Since im- and exports as well as storage are not being modeled, it should not be evaluated with national standards.

The reduction in load shedding was achieved by additional dispatch of conventional generation. If there are no flexible generators, 12.8% additional conventional generation must be scheduled. From 60% flexible share, the additional dispatch is 5.9%. Above 40%, the dispatch of inflexible power plants no longer differs between deterministic and stochastic day-ahead clearing.

The increased dispatch of inflexible power plants increases curtailment with low installed flexibility. This disadvantage disappears for flexible shares greater than 30%. A minimum curtailment of 22.7% of the total annual potential wind feed-in (or 13.1% of total annual demand) remains even at 100% flexible share. Intraday clearing may even increase curtailment slightly.

It was found that the upward and downward corrections in stochastic intraday clearing are already maximized at 30% flexible share. The maximum is 0.6% (of the total annual demand) upward corrections and 3.2% downward corrections, which then reduce asymptotically to 0.1% and 1.6% as the flexible share increases. In deterministic intraday clearing, both upward and downward corrections increase asymptotically to 3.3% and 3.4% of the total annual demand.

The development of the intraday corrections was put in relation to the magnitude of the forecast errors that can be compensated for by intraday clearing. The amount of annual intraday corrections behaves asymptotically. This means that the amount of available intraday flexibility is large enough to compensate for the largest possible forecast error. Downward corrections are larger in stochastic clearing than in deterministic clearing. This shows that the additionally scheduled flexible generation is not necessarily required.

4.2.2 Sensitivity to extra costs in balancing

Flexible generators are assumed to charge an extra fee for providing short-term flexibility. This is represented by parameters κ^+ and κ^- (first introduced in equation 2.3) for purchase and repurchase cost extras, respectively. The deterministic dispatch is unaffected by cost extras and their variation affects only the intraday clearing or balancing results. The stochastic clearing anticipates balancing measures, and thus, adapts its day-ahead dispatch to these costs as well. To keep total costs constant, κ^+ and κ^- were adjusted simultaneously. Assuming that the amount of positive forecast error (when DA $\leq$ ID) is equal to the amount of negative ones (when DA $\geq$ ID), decreasing the cost of upward correction while simultaneously increasing the cost downward corrections should not affect the average annual operating costs. The results are compared against the ratio of extra fees charged for purchase and repurchase measures – short up-to-down ratio R. 50% of conventional capacity installed is flexible.

Figure 4.14 shows the total costs from deterministic clearing are hardly affected by the increase of the up-to-down ratio. Total costs increase from 2.875 €/MWh to 2.886 €/MWh without short-term corrections. Intraday clearing decreases costs overall but is also subject to an increase from 2.040 €/MWh to 2.051 €/MWh. Total costs increase with R as there are slightly more purchase than repurchase actions per year.

The stochastic total costs on the other hand decrease with increasing up-to-down ratio from 1.827 to 1.755 €/MWh. Including intraday clearing reduces costs further by around 0.07 €/MWh. Two effects reduce the total costs. Firstly, costly upward corrections are reduced and secondly,

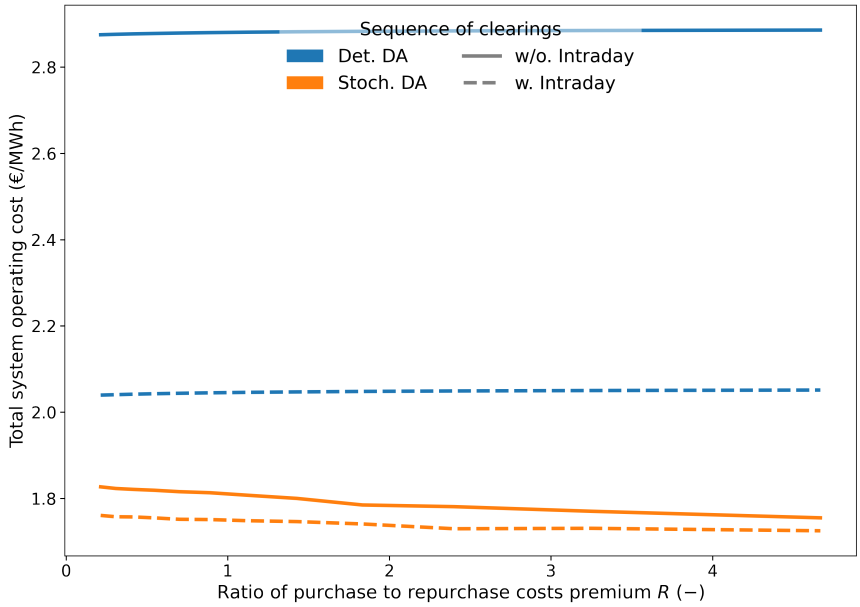

Figure 4.14: Sensitivity of total operating costs against the up-to-down ratio R. Deterministic and stochastic clearing are compared with and without intraday clearing.

load shedding is reduced. Both effects are linked closely as they stem from higher day-ahead dispatch of OCGT generators.

Figure 4.15a illustrates how an increase in annual total day-ahead dispatch of OCGT generators leads to a decrease in total annual load shedding which is shown in figure 4.15b. The total day-ahead dispatch increases linearly with the up-to-down ratio. The total day-ahead dispatch at $R = 0.21$ is 57.04% of the total annual demand. This increases up to 61.12% if purchase extra fees exceed repurchase fees by a factor of five. The share of nuclear generation decreases slightly, but OCGT generation is increased strongly. Load shedding halves without intraday from 0.072% to 0.035% of total annual demand. The reduction in shedding after intraday clearing due to the increase in the up-to-down ratio is smaller, falling from 0.028% to 0.012%.

$$E^{+/-} = \sum_{t=1}^{8760} \sum_{n,s} G^{+/-}_{n,s,t} \tag{4.7}$$

This increase in day-ahead dispatch clearly affects the total annual amount of balancing measures (see equation 4.7) as shown in figure 4.16. Without intraday clearing, upward corrections reduce from 2.43% of total annual demand at $R = 0.21$ down to 0.76% at $R = 4.67$. With intraday clearing, the volume of balancing measures decreases from to 2.07% to 0.71% of total demand. If the up-to-down ratio is small, the absolute and relative impact of intraday clearing is larger than at large values of R. This is due to increased dispatch in the day-ahead clearing under high purchase costs in balancing.

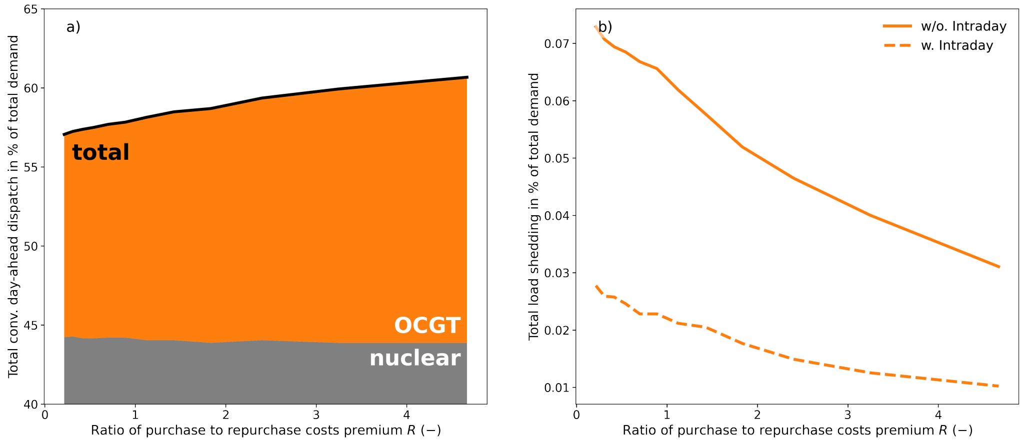

Figure 4.15: Sensitivity of total annual conventional day-ahead dispatch (a) and total annual load shedding (b) to the up-to-down ratio R. The impact of intraday clearing on load shedding is also included.

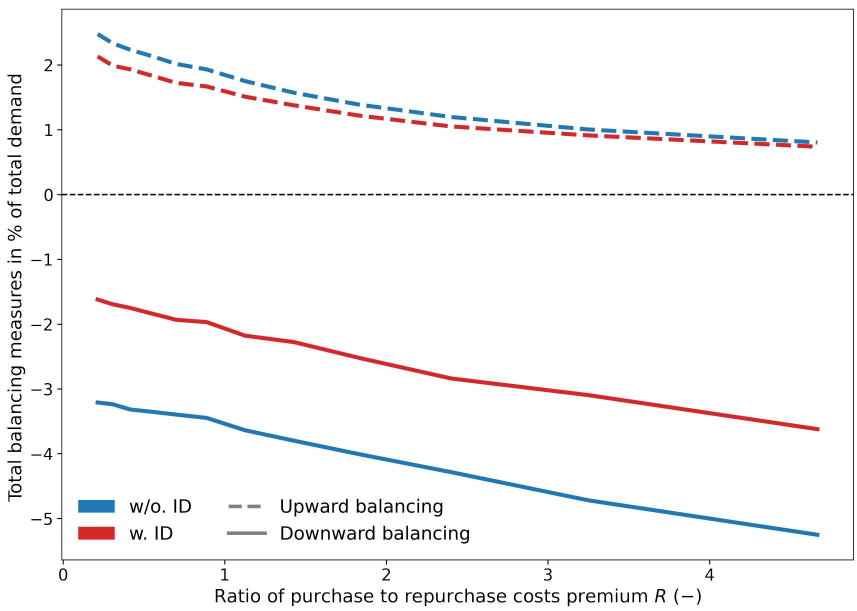

Figure 4.16: Sensitivity of total annual balancing measures of OCGT generators performed against up-to-down ratio R. Balancing measures without intraday clearing (represented by blue colour) are compared to those required after intraday clearing (represented by red colour).

The total amount of downward balancing increases with the up-to-down ratio. Without intraday clearing, 3.14% are reduced at $R = 0.21$ and 5.25% at $R = 4.67$. Intraday clearing reduces the amount of downward balancing overall. Now balancing measures increase from 1.57% at $R = 0.21$ up to 3.57% at $R = 4.67$. The slope with intraday corrections is slightly less steep.

While the development of upward balancing with the up-to-down ratio followed a somewhat asymptotic behavior, downward corrections increase linearly in absolute terms.

The extra amount of day-ahead dispatch of OCGT generation is now compared to the amount of load shedding and intraday purchases. This comparison is based on the observation that load shedding, although slightly increased for $R = 0.21$, is very low if stochastic dispatch is used. Therefore the uncertainty information available is used differently for low and high purchase costs at delivery.

The reduction in upward balancing required reduces by 1.67% while day-ahead dispatch increases by 3.52%. The volume of downward balancing increases by 2.11% (with ID 2.00%). At $R = 0.21$, it is less efficient to plan for more security, as downward balancing is expensive while upward corrections are cheap. Hence, the day-ahead dispatch there covers scenarios where anticipated balancing measures are too large to be carried out only at the delivery. Further events do not experience higher day-ahead dispatch as balancing down is potentially too expensive. In this case, 2.4% of extra generation have to be added during balancing at the delivery. On the other hand, at $R = 4.67$, upward balancing is very expensive, and thus, procurement of generation capacity early on is more efficient. Only events where anticipated balancing measures are small and less likely to occur are not covered by the additional dispatch. In this case, 0.76% of upward balancing are required. Hence, including a large portion of uncertainty information leads to a decrease in upward balancing of 1.67%. To achieve this, 4.08% of additional day-ahead capacity are procured. In the end, in terms of load shedding, almost the same result was achieved as load shedding only reduces by an extra 0.027%, yet uncertainty information was weighted less.

4.2.2.1 Analysis of high-risk events

This illustrates how identical forecast information leads to different dispatch results, depending on the risk posed by balancing costs. The system tends to plan for more excess capacity if the anticipated risk is increased. The excess is then not fully utilized to reduce balancing measures or load shedding. This observation raises the question which events pose sufficient risk of load shedding, despite low balancing costs, to warrant an increased day-ahead dispatch. In section 4.1.2, scatter plots were used to study the impact of wind farm forecast median and spread on the dispatch of the flexible generator G1 in the day-ahead clearing. Similarly, the aggregated day-ahead dispatch of OCGTs $P_{\mathrm{OCGT},t}$ could be scattered against the aggregated day-ahead forecast median of all wind farms $\mathrm{FC}_{\Omega=\mathrm{DA,median}}$ in the five-node network. In equation 4.8a, the OCGT DA dispatch $G_{n,\mathrm{OCGT},t}$ is aggregated over all nodes. The sum is divided by the total nominal installed OCGT generation capacity (take tab. 3.7 with 50% share of OCGT) for the sake of simplicity and comparability. In equation 4.8b, the day-ahead forecast median $q_{0.5}$ of each wind farm is calculated, weighted by its nominal capacity and then summed over all wind farms. The sum is divided by the total nominal installed wind farm capacity. With these simplifications, it is assumed that the five-node network operates as if it had a single OCGT and wind farm. The hourly resolved aggregated electricity demand of the system as defined in equation 4.8c serves as the only system load.

$$P_{\mathrm{OCGT},t} = \sum_n \left[G_{n,\mathrm{OCGT},t} \cdot \bar{G}_{n,\mathrm{OCGT}}\right] / \sum_n \bar{G}_{n,\mathrm{OCGT}} \tag{4.8a}$$

$$\begin{aligned} \mathrm{FC}_{\Omega=\mathrm{DA},\mathrm{median}} = \sum_n \Big[& q_{0.5}\left(\tilde{G}_{n,\mathrm{onwind},t,\omega}, \Omega = \mathrm{DA}\right) \cdot \bar{G}_{n,\mathrm{onwind}} \\ & + q_{0.5}\left(\tilde{G}_{n,\mathrm{offwind},t,\omega}, \Omega = \mathrm{DA}\right) \cdot \bar{G}_{n,\mathrm{offwind}} \Big] \\ & / \sum_n \left[\bar{G}_{n,\mathrm{onwind}} + \bar{G}_{n,\mathrm{offwind}}\right] \end{aligned} \tag{4.8b}$$

$$d_t = \sum_{n,i} D_{n,i,t} / \max\Big(\sum_{n,i} D_{n,i,t}\Big) \tag{4.8c}$$

Scatter plots are generated for both $R = 0.21$ and $R = 4.67$ and compared to each other. The difference between both diagrams is related entirely to the impact of the up-to-down ratio. It is to be expected from figure 4.15a that the DA dispatch of OCGT will reduce overall for $R = 0.21$. The following investigation shall provide an insight into how the dispatch is reduce at an hourly resolution. It is tested whether a group of events which do not change under cost reduction can be identified.

Figure 4.17 shows the above introduced scatter plots of aggregated OCGT DA dispatch against the aggregated DA forecast median. A colorbar with six shades has been added to provide information on the system demand. I do not attempt to explain every detail of both diagrams as I do not have an in-depth grasp on the system dynamics. Furthermore, it is obvious that this simplified view does not provide an insight into the impact of network constraints but may still be useful to identify events which are affected.

Figure 4.17a shows the results for a low up-to-down ratio of $R = 0.21$. Starting at a high demand, OCGT dispatch is large if the forecast median is small. Dispatch of OCGTs is negatively proportional to the system demand for most events up to 20% of the forecast median. Beyond 20%, OCGTs only react proportional to the forecast median if system load is above 90%. In many cases, day-ahead dispatch of OCGTs is zero. For low forecasted wind feed-in, this occurs mostly at small loads, while for high forecasted wind feed-in it also occurs for events with high demand above 80%. Another characteristic is a series of events where the total OCGT dispatch is at 40% of nominal capacity (see collection of points at 40%). Other events scattered in the field between 50 and 100% of forecast median and 0 to 40% of OCGT dispatch do not follow a clear pattern. In the region where the demand is high and the forecast is low, the system behaves almost deterministically. Also events with zero dispatch corresponding to events where wind forecast is large enough to not plan for security, can be viewed as behaving in a deterministic way. To clarify, *deterministic behaviour* in this regard means that the dispatch follows a merit

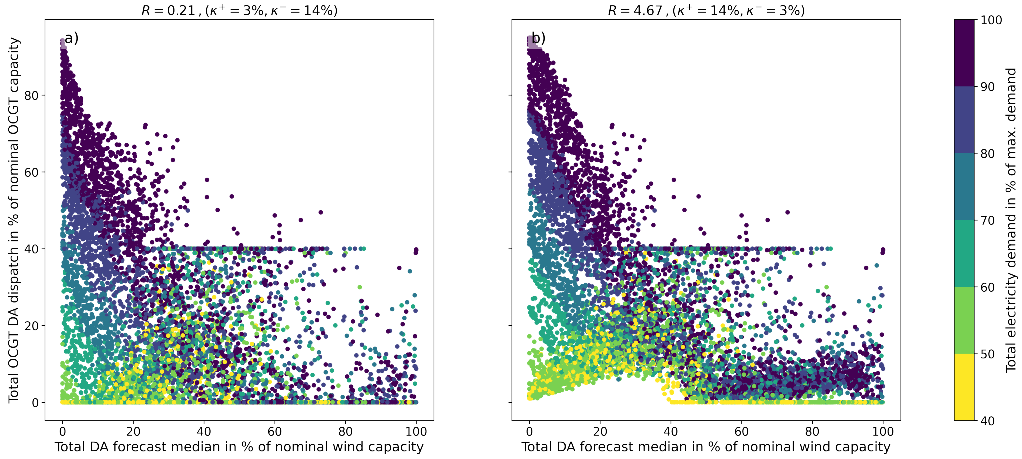

Figure 4.17: Aggregated day-ahead dispatch of OCGT generators with respect to the aggregated day-ahead forecast median of all wind farms compared for low up-to-down ratio in (a) and high up-to-down ratio in (b). Each dot represents a single hour. The demand per hour has been aggregated and sorted into six bins to be displayed as a colormap.

order where the dispatch of gas turbines is defined by a single forecast parameter like mean or median like in the deterministic clearing. In section 4.1.2, a non-deterministic behaviour was discussed where the dispatch of flexible producer G1 was proportional to the forecast spread. Non-deterministic dispatch occurs for the line of events with 40% dispatch and in the region which does not follow a distinct pattern. Also increased dispatch of OCGT for a demand of less than 50% at 30% forecast median would not appear in deterministic clearing.

Figure 4.17b on the other hand shows the results for a high up-to-down ratio of $R = 4.67$. Again starting at a high demand and low predicted wind feed-in, OCGT dispatch is negatively proportional to the forecast median. This proportionality breaks at last at 30% forecast median for events with a demand less than 90%. For events with a demand less than 60%, the dispatch of OCGTs grows proportionally with the forecast median. Beyond 40% of forecast median, events with small load experience zero dispatch of OCGT. In this range of high forecast median, events with load above 70% have an OCGT dispatch that grows proportionally with forecast median. Low and high demand events are clearly separated here. There is a series of events at which have a dispatch of 40% regardless of the wind forecast, which mostly occur above 80% of demand. Comparing figures 4.17a and b, similar structures can be identified. The range where OCGT dispatch is negatively proportional to forecast median appears in both data sets but is shifted upward for $R = 4.67$ (compare 10% forecast median and 80% OCGT dispatch in both figures). There is also a series of events at high wind forecast where OCGT is not dispatched. For $R = 0.21$ both low and high demand cases may have zero dispatch, if R is increased to 4.67, only low demand cases remain. Lastly, the series of events with precisely 40% OCGT dispatch is found in both model runs. They additionally have a number of events which lie outside of the proportionality found at high demand and low forecast in common. The strongest difference is found in the positive proportional correlation between low demand events at low forecast levels and high demand events at high forecast levels which only appears for $R = 4.67$.

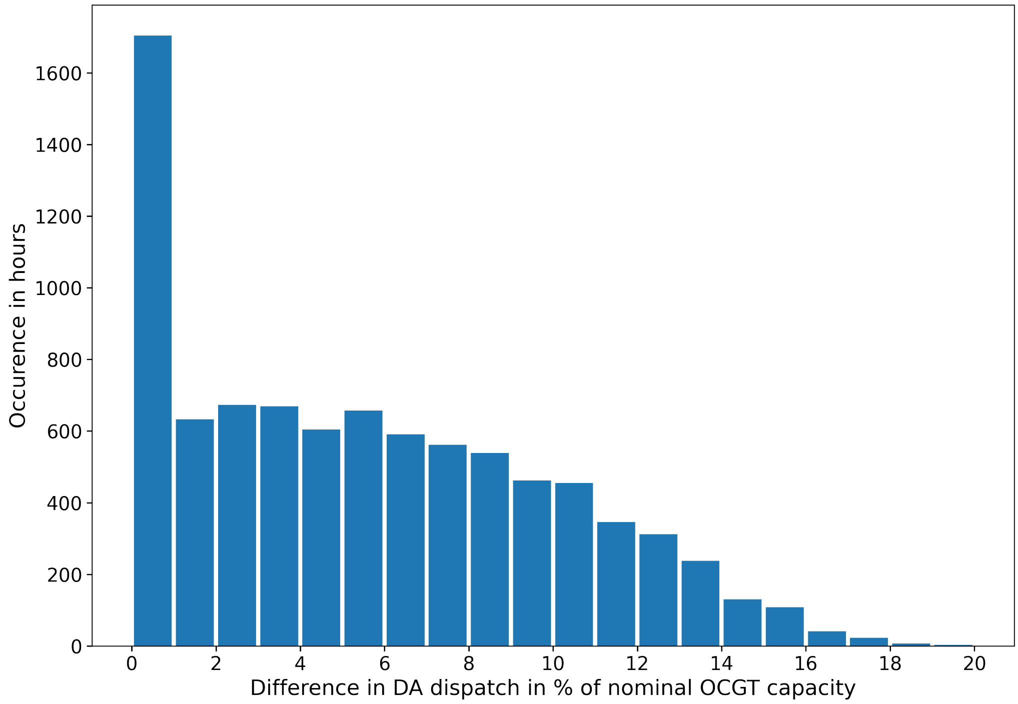

Figure 4.18: A histogram of the occurrence of events where the total day-ahead dispatch of OCGT generators changes by a set amount due to changes in the up-to-down ratio. Events in hourly resolution of the year 2021 have been sorted into bins of 1% width.

To quantify the difference between both model runs more in detail, the difference of the aggregated OCGT day-ahead dispatch for $R = 0.21$ and $R = 4.67$ is determined. The differences have been sorted into bins of 1% width and the number of occurrences are presented in figure 4.18. In 1680 events the total OCGT dispatch is changed by less than 1% of nominal capacity when ramping costs are adjusted. In a wide range of about 3600 events the dispatch is varied between 1 and 7%. Above 7%, the number of events registered by difference in dispatch decreases with the magnitude of the difference. The largest difference is about 20%. The sum over the differences in dispatch larger than 1% accounts to a total dispatched OCGT energy of 5622956 MWh, or 4% of annual total electricity demand. This is roughly equal to the difference of 4.08% identified in figure 4.15a when comparing the total day-ahead dispatched energy at $R = 0.21$ and $R = 4.67$. While load shedding decreases with the up-to-down ratio, even at an R value of 0.21, it remains significantly lower than the amount observed in deterministic clearing (see figure 4.10 for comparison at 50% share of OCGT). Therefore, events in which OCGT dispatch changes by less than 1% between both ramping cost configurations can be attributed to the decrease in shedding events when comparing stochastic and deterministic clearing.

These events have been isolated in figure 4.19 which shows only the data points for $R = 4.67$, i.e. the configuration of ramping costs used throughout the remainder of this report, where above discussed events with less than 1% change in dispatch have been highlighted. The marked events spread across a wide range of predicted wind power feed-in. At a low wind forecast between 10 and 30%, mostly events with high demand larger than 80% are marked. Above 40% wind power forecast, also events with a demand less than 70 or even 60% are found. A large group of low demand events remains constant at zero OCGT dispatch if day-

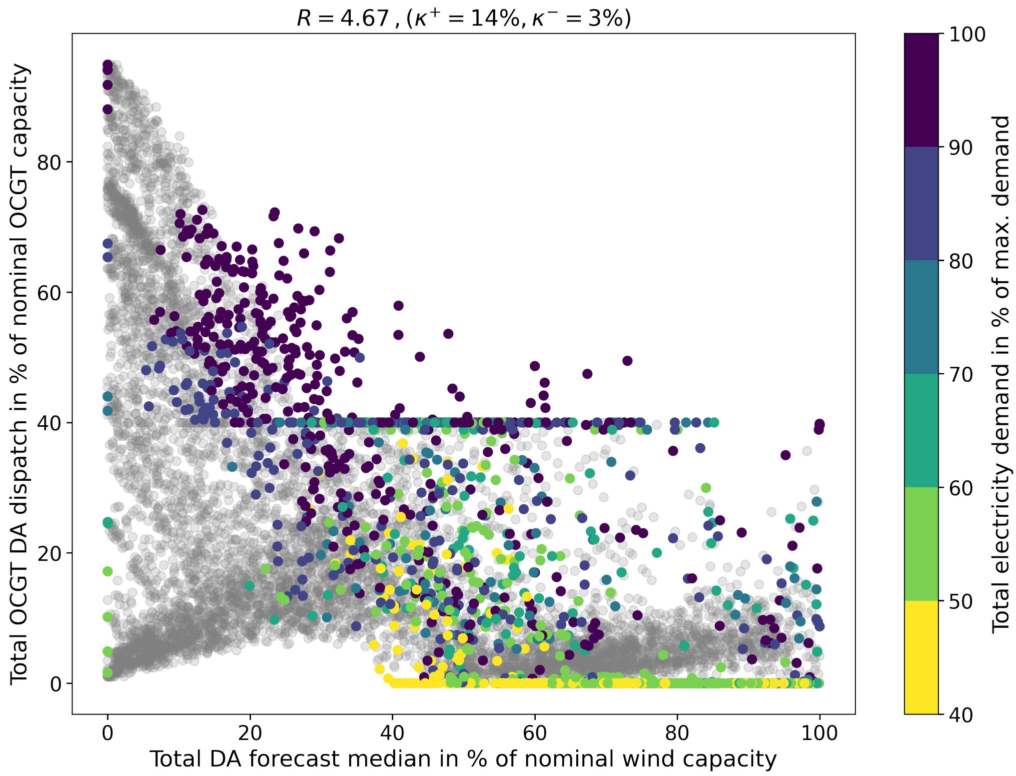

Figure 4.19: Aggregated day-ahead dispatch of OCGT generators with respect to the aggregated day-ahead forecast median of all wind farms at an up-to-down ratio of $R = 4.67$ in hourly resolution. Events which do not change if R is reduced to 0.21 are highlighted.

	Shedding hours	Total demand shedding per total demand
det. DA (full year)	839	0.788%
det. DA (highlighted)	189	0.247%

Table 4.3: Comparison of demand shedding results for deterministic clearing in general (*full year*), and limited to only those events which do not change (*highlighted*) in stochastic clearing when the up-to-down ratio is varied.

ahead forecast is larger than 40%. Events with less than 60% of maximum demand occur mostly beyond 80% wind power forecast. If the wind forecast is greater than 30%, events with high demand often have an OCGT dispatch of 40% of its nominal capacity.

This investigation has been started as it was assumed that the highlighted cases account for a large share of reduced load shedding. It has been noted that load shedding is vastly reduced compared to deterministic clearing even if the additional OCGT reserve is kept small, due to the reduction of purchase costs for balancing. This hypothesis shall now be tested. Therefore table 4.3 contains the amount of shedding hours and total load shedding for the deterministic clearing without intraday corrections (*full year*). The second row of entries uses only events which have been *highlighted* in figure 4.19. It is expected that events with non-zero dispatch have high expected balancing costs due to anticipated load shedding. The *highlighted* events are used as a mask on the deterministic data set, to check the amount and hours of load shedding covered within these events.

The *highlighted* events account for one quarter of the shedding hours in deterministic clearing.

could be identified and these account for roughly 1/3 of the total load shedding. The events that have been identified Not all events could be identified which are at the risk of load shedding in deterministic clearing. The dispatch of these events is not at its maximum if purchases at delivery are cheap.

Nonetheless, this analysis has helped to identify events which are of high importance when reducing load shedding. OCGT dispatch has been added to events which have been identified above as being proportional to the forecast median even though they are not strictly required to reduce load shedding. While it does help to reduce load shedding and short-term upward corrections during balancing, it does so with limited success as discussed when comparing figures 4.15a and 4.16.

The range of events at 40% OCGT dispatch is likely connected to events where the spread is high or where there are outliers in the forecast ensemble. As the total OCGT DA dispatch is at 40% of it nominal capacity, this must mean that this issue is prevalent in all large wind farms across the nodes. This interpretation is derived from section 4.1.2 where events with 30 to 40% regardless of spread or day-ahead median where identified to have a heavy tail distribution. This means that most members predict the same outcome yet some predict a different path. This poses a large risk if the system demand is high.

Events which break out of the deterministic behavior for high demand between 10 and 30% DA median are probably caused by transmission capacity constraints. If the demand throughout the system is high, and the wind feed-in for example from wind farms in the North is large, then the network may be congested. Such a congestion is then countered by an increased dispatch of generators per node.

4.2.2.2 Conclusion

In this study, the cost extras that generators demand for the provision of flexibility in balancing and intraday clearing were each adjusted in twelve steps and the effect on total system costs, day-ahead dispatch, load shedding and balancing measures were considered. Only the ratio of purchase to repurchase-extra R, known as the up-to-down ratio, was of significance in the analysis.

All parameters increase or decrease monotonically with increasing up-to-down ratio. Therefore, only values for $R = 0.21$ and $R = 4.67$ are explicitly stated. Total costs from deterministic clearing increase slightly from 2.875 €/MWh to 2.886 €/MWh without intraday corrections (with intraday clearing minus 0.830 €/MWh). The increase shows that there are more upward corrections than downward corrections in balancing.

In stochastic clearing, the total system costs decrease from 1.827 €/MWh to 1.755 €/MWh (with intraday clearing minus 0.070 €/MWh). The reduction in costs can be attributed to the reduction in load shedding. This is halved from 0.072% to 0.035% of the total annual demand without intraday clearing (with intraday clearing from 0.028% to 0.012%).

This reduction is due to the increased day-ahead dispatch of flexible conventional generators with rising R. At $R = 4.67$, the day-ahead dispatch of OCGTs is 4.08% of the annual demand higher than at $R = 0.21$. Compared to the deterministic day-ahead dispatch of 54.0% of the annual demand by conventional power plants, even with low anticipated balancing costs, 57.08% (i.e. an additional 3.08%) is still covered by conventional generators. This ensures a drastic reduction in shedding compared to deterministic clearing.

Without intraday clearing, upward corrections of 2.43% and downward corrections of 3.14% of the total annual requirement are necessary at $R = 0.21$ in balancing. The upward corrections fall to 0.76% at $R = 4.67$ and the downward corrections to 5.25%. Intraday clearing reduces both upward and downward corrections in absolute terms.

It was discussed in more detail that the additional scheduled flexibility on the day-ahead is not fully utilized to reduce balancing measures. From this analysis, 1680 events were identified for which, even with very low costs for upward corrections, no change to the day-ahead dispatch takes place. Both events that were not scheduled on the day-ahead, and events with greatly increased dispatch where identified. The events (stochastic, no change in dispatch when costs change) were compared to events in deterministic clearing without intraday where load shedding occurs. This way 22.5% of shedding hours and 31.3% of the demand shed were identified in the data set from deterministic clearing. The identified events account for events in deterministic clearing with strong shedding.

4.2.3 Sensitivity to cost discount in intraday clearing

Producers operating in the intraday clearing, offer corrections to the dispatch at a reduced cost compared to the costs during balancing. Stochastic intraday clearing anticipates consequences on balancing, a cost discount in the intraday clearing might therefore impose an incentive to clear corrections before balancing. Deterministic clearing is expected to remain unaffected by changes in the cost discount in the intraday clearing.

It is not clear, whether this discount provides an incentive of its own to perform intraday corrections compared to the predominant role of the flexible share (see section 4.2.1.5). This question is investigated for both deterministic and stochastic clearing for two OCT shares. The driving parameter will be the premium factor ϱ which has been introduced in equation 2.7. It defines the difference between intraday and balancing costs. If $\varrho = 0$, then the intraday costs are identical to the day-ahead marginal costs $\mathbf{C}^{+/-,*} = \mathbf{C}$. If the premium is increased to $\varrho = 1$, then intraday and balancing costs are equal $\mathbf{C}^{+/-,*} = \mathbf{C}^{+/-}$. The discount of intraday clearing with respect to balancing costs and is defined as $1 - \varrho$. The results discussed so far were obtained at a discount level of 20%.

Figure 4.20 shows the change in total system operating costs with respect to the cost discount on intraday corrections $1 - \varrho$, which was varied between 0% and 100%. If the discount increases from 10 to 99%, the total costs from deterministic clearing decrease by 0.008 €/MWh regardless of the flexible share. In stochastic clearing, costs increase slightly by 0.003 €/MWh to 2.496 €/MWh at 30% flexible share, and more drastically from 1.633 to 1.673 €/MWh at 100% flexible share. 100% is considered as an outlier since the amount of intraday corrections

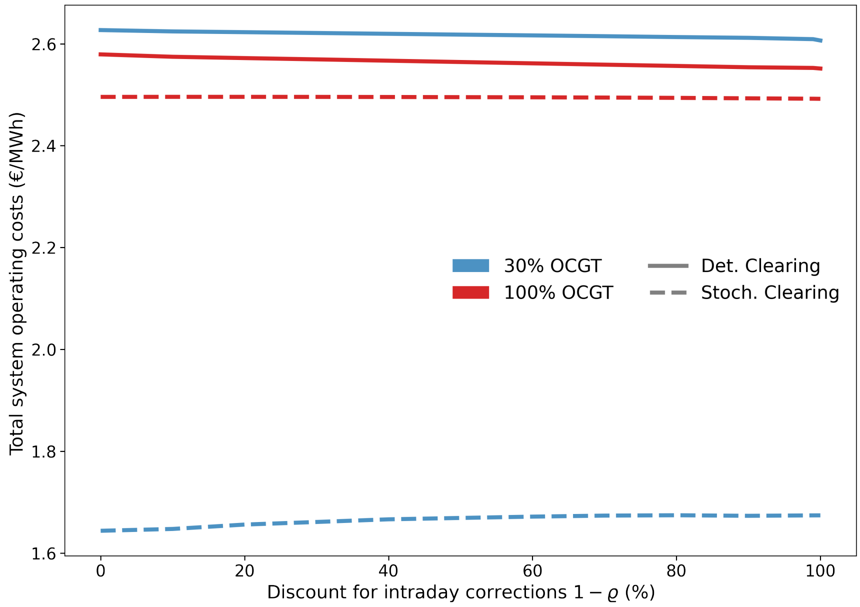

Figure 4.20: The sensitivity of total operating costs with respect to the discount on intraday costs $1 - \varrho$. Deterministic (represented by solid line) and stochastic clearing (represented by dashed line) are being compared at 30% and 100% share of installed OCGT per total conventional generation capacity.

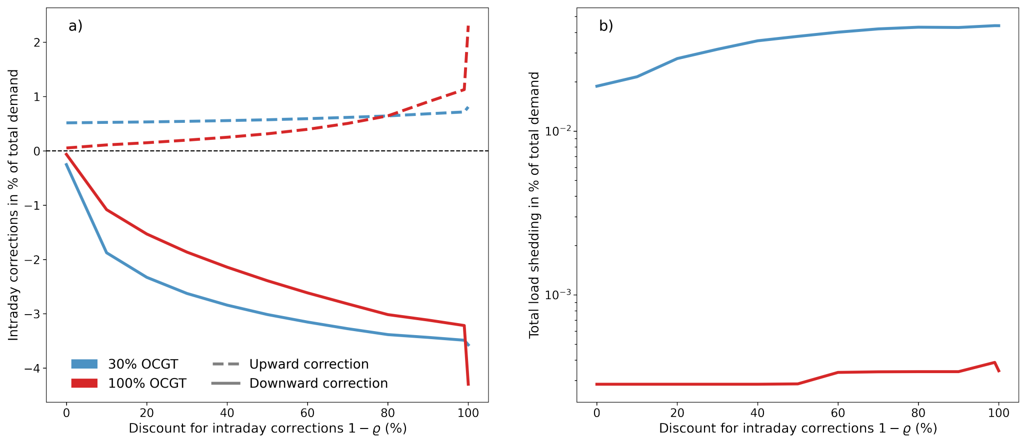

Figure 4.21: The sensitivity of total annual intraday corrections with respect to the discount on intraday costs $1 - \varrho$ for stochastic clearing (a) is compared to the resulting load shedding (b). The sensitivity is studied at 30% and 100% share of installed OCGT per total conventional capacity.

increases drastically from 99% to 100% even though the change in costs for corrections is tiny. There is no effect on total system operating costs.

As the deterministic intraday does not have any information of the consequences of its corrections on balancing measures, a change in the discount $1 - \varrho$ will not affect dispatch solutions and only affect the total system operating costs. This expectation is supported by figure 4.20. Hence, only stochastic clearing, with its rather unexpected increase in total costs will be analyzed. Figure 4.21a shows the total intraday corrections against the cost discount for them. The effect on load shedding is added in figure 4.21b.

Figure 4.21a shows the sensitivity of intraday corrections with respect to the intraday discount $1 - \varrho$ for 30 and 100% share of OCGT. At 30% OCGT share, intraday upward corrections rise slightly from 0.6% to 0.7% if the discount is increased from 0% to 99%. Compare to that, the intraday corrections at 100% OCGT share. At 0% discount, the intraday purchases are at 0.05% of the total demand which then increase up to 1.1% if the discount is at 99%.

For 30% OCGT share, upward corrections are required even if no discount is provided by intraday clearing. This shows that the day-ahead dispatch is not sufficient to compensate for any forecast update in general. The stochastic intraday anticipates balancing costs too, and thus, if the available flexible dispatch cannot the react to the changes by all forecast members, additional flexibility has to be procured. In other words, this means that upward corrections to the day-ahead dispatch occur if the expected cost from load shedding is larger than the extra cost from the dispatch of flexible generators. This is different to deterministic intraday clearing where simply the mismatch between intraday forecast and day-ahead dispatch would be equalized. The scale of the cost advantage over the corrections performed during balancing determines how strong the flexible generators respond.

For 100% OCGT share and zero discount, no intraday corrections are performed. Compared to the low flexibility case, this shows that the day-ahead dispatch is robust enough to balance out the forecast deviations. Nonetheless, intraday upward corrections increase with the discount. This can be explained by the expected reduction of load shedding through extra procurement of OCGT capacity.

For both shares of flexible generation, intraday repurchases increase in absolute terms. These repurchase events generally occur when the intraday forecast has predicted more wind than dispatched in the day-ahead clearing. At zero discount, 0.18% and 0.08% of the total annual demand are repurchased at low and high flexible share, respectively. This shows that if intraday corrections are as expensive as balancing measures, there is no advantage in reducing the dispatch before delivery. This amount of downward corrections increases to 1.8% and 1.1% at low and high flexible share, respectively, if the discount is increased to 10%. When the discount is increased to 99%, the total amount of downward corrections increases up to 3.5% and 3.0% for low and high flexible shares, respectively. This increase in downward corrections simply confirms that the day-ahead dispatch plans for some flexible reserve. If not required, the reserve capacity is repurchased during balancing. The system operator receives less money than paid before during day-ahead dispatch. Intraday clearing also provides the option to repurchase flexible reserve capacity, however, at a reduced cost (as explained above). Repurchasing, not required, extra capacity in the intraday clearing reduces the expected balancing costs.

However, a decrease in flexible generation capacity corresponds an increased risk for shedding events during balancing as forecast error may not be balanced out sufficiently anymore. Interestingly, it is observed that load shedding increases for both low and high flexibility when the cost discount from intraday clearing increases. This is shown in figure 4.21b where load shedding at low flexibility rises from 0.02% to 0.04%. Even though additional generation is procured, the increasing repurchase of OCGT capacity results in a rising risk for forecast errors to cause load shedding. The system is more sensitive to errors in the intraday forecast if the discount is increased.

4.2.3.1 Conclusion

The premium factor ϱ (which defines the cost of intraday corrections with respect to the costs for balancing measures) affects total system operating costs by changing the total amount of intraday corrections and load shedding both at 30% and 100% flexible generator share. It has been reinterpreted as the discount factor $1 - \varrho$, which describes the cost discount with respect to the costs for balancing measures.

Total system operating costs in deterministic clearing are reduced by 0.008 €/MWh for both levels of flexibility when increasing the discount. In stochastic clearing, however, the discount increased the total system operating costs for both levels of flexible share. At 30%, the costs were increased by 0.040 €/MWh. For zero discount and 30% flexible share, the stochastic intraday clearing still performs upward corrections of 0.6% of the total annual demand, which increase to 0.7% of the total annual demand if the discount is increased to 100% (corrections cost as much as day-ahead dispatch). At 100% flexible share, the amount of upward corrections increases with the discount. At zero discount, upward corrections of 0.05% of the total annual demand are performed which increase up to 1.1% at 99% discount. The difference between low and high flexible share was explained by the capability of the day-ahead schedule to compensate for deviations between day-ahead and intraday forecast.

The amount of downward corrections increases with the discount regardless of the flexible share. At 30% flexible share, 0.18% of the total annual demand is corrected down at zero discount, and 3.5% at 100% discount. The corrections are slightly decreased in absolute terms if the flexible share is at 100%. The total amount of load shedding increases with the discount for intraday corrections for both flexible shares. It was explained by the risk imposed by reducing the flexible reserve for balancing through downward corrections which are increased by the discount.

Chapter 5

Conclusion

The uncertainty of power forecasts was integrated in the form of probabilistic wind power forecasts into the sequence of day-ahead and intraday market clearings using the Probabilistic Power Forecast Evaluation Tool (ProPower). Integrating uncertainty into economic dispatch reduces operating costs, curtailment and load shedding which are used as key indicators. The *deterministic* clearing approach uses deterministic forecasts where dispatch does not account for potential balancing costs. This approach was compared to the *stochastic* clearing which provides a dispatch that is optimized to reduce operating costs and potential / expected balancing costs. The intraday market clearing has been implemented to enable wind power plants to correct their dispatch based on short and shortest-term forecast updates.

A simple two-node power network with a single wind power plant, and a five-node network with eight have been studied. Probabilistic forecast data from the ECMWF Ensemble Prediction System were used as day-ahead and intraday forecasts. The amount of required balancing was determined by the deviation of forecasted wind power to feed-in computed from ERA5 reanalysis data. The two-node network received data from the location of Nordergründe, and the five-node network included data of further locations in the West of Germany.

A comprehensive sensitivity analysis of ProPower was carried out on the five-node network. First, the sensitivity of several key indicators on the share of installed flexible generators in the total conventional generation capacity (short *flexible share*) was studied. Second, the sensitivity to the ratio of cost extras charged for corrections in intraday clearing and balancing with respect to day-ahead costs was investigated. And lastly, as the intraday corrections are assumed to be offered at a discount with respect to balancing, it was investigated whether the the cost discount by generators acts as an incentive to clear more intraday corrections.

A power system managed by stochastic clearing reduces the total amount of load shedding in the five-node network at 30% flexible share from 1.5% (deterministic clearing) to 0.06% (stochastic clearing) of the total annual demand. Increasing the flexible share to 100%, the stochastic clearing still outperforms deterministic clearing with 0.001% versus 0.1%. Curtailment is reduced by up to 1.2% through stochastic clearing, when the flexible share is greater than 30%.

Uncertainty information from probabilistic forecasts is used to procure a flexible reserve which may be activated during balancing. In the simple two-node network, the dispatch of the flexible generator is proportional to the inter-quartile range of the probabilistic wind power forecast. Reducing the prob. information to the inter-quartile range, however, is not sufficient. It was shown that load shedding was prevented by a strongly asymmetric ensemble forecast leading to an increased dispatch of the flexible generator. Here, the inter-quartile range was very small. The correlation between forecast inter-quartile range and dispatch of flexible generators gets blury in the five-node network when more complex load profiles are considered. This has been shown in a scatter plot of flexible generator dispatch against the wind power forecast median. The procurement of a reserve still persists with 12.8% additional dispatch at zero flexible share, and 5.9% more at 100% flexible share. The deterministic clearing results in a constant total conventional dispatch of 54% of the total annual demand. The dispatch of inflexible generators is not reduced to make room for more wind power feed-in in stochastic day-ahead clearing in general. Actually, the dispatch of inflexible generators is even increased to ensure the security of supply at low flexible shares.

Sufficient procurement of flexible reserves in the day-ahead clearing undermines the value of short-term forecasts to the system. When procuring a reserve through stochastic day-ahead clearing, short-term forecast updates in the intraday clearing hardly affect the annual system performance. The maximum additional reduction of load shedding was 0.02% of the total annual demand through stochastic intraday clearing at 30% flexible share. This is marginal in comparison to deterministic clearing, where load shedding is reduced by an additional 0.84% of the total demand through intraday clearing. This shows that without a very high flexible reserve for balancing, deterministic clearing benefits strongly from corrections through short-term forecasts. This benefit is even amplified when the flexible share is lower than 30%.

Therefore, under the selected restrictive ramping constraints, it is the ability to handle extreme forecast errors, rather than the reduced cost of correcting generator dispatch errors in general, that reduces total system costs through intraday clearing. When the discount of intraday corrections over balancing measures increases, total system costs may even increase in stochastic clearing. In the five-node network with 30% flexible share, the total system costs increased by 0.040 €/MWh if the intraday correction costs are reduced from full balancing to day-ahead costs. The flexible reserve was being reduced by an increasing amount of repurchases, leading to a higher risk for costly load shedding.

The procurement of flexible reserves in the day-ahead clearing is determined by cost extras expected for balancing. Throughout this work, the cost extra for upward corrections was 4.67 times larger than the extra for downward corrections. If the ratio is inverted, the non-wind day-ahead dispatch decreases by 4.08% (of the total annual demand) to 57.04%. Load shedding increases to 0.072% of the annual demand but is still much smaller than shedding for deterministic clearing which is 0.9%. This shows that the same uncertainty information may lead to quite different dispatch results which still prevent large shares of the load shedding.

Events have been identified where the day-ahead dispatch is not decreased, despite upward corrections in balancing being less expensive than downward ones. These events showed an increased dispatch of flexible generators, which was attributed to precautions against possible load shedding.

Intraday clearing makes it possible to analyze short-term forecasts with a higher forecast skill by comparing, for example, total system costs, load shedding or curtailment for different forecasts. One could study improved forecasts both on a system-wide or local level. LIDAR shortest-term forecasts of individual wind farms have been developedTheuer et al., 2020 for short lead times of less than 15 minutes. These impact of LIDAR forecasts is explored in the project *WindRamp*.

As stochastic intraday clearing only leads to a comparatively small system-wide improvement, it is to be expected that the gain from improved probabilistic short-term forecasts in the given model will be small. However, it is to be expected that individual operators will certainly benefit from improved forecasts, as they will be able to offer their dispatch more reliably. An evaluation from the operator's perspective (e.g. through revenues) could be helpful to better emphasize the high value of probabilistic information.

At present, flexible generators provide the system with the necessary capacity for corrections in balancing. It is expected that energy storage systems will offer a large part of this flexibility in the decarbonized supply of the future. Therefore, one should investigate whether probabilistic forecasts are still more valuable than deterministic forecasts if storage facilities are available in sufficient (ramping) capacity. Assuming stochastic day-ahead clearing, it will be interesting to investigate, if the use of probabilistic information leads to less storage capacity required than when using deterministic forecasts only. The discussion of storage systems should be coupled to an implementation of solar power which provides substantial feed-in in the diurnal cycle.

Bibliography

Ahmed, A., & Khalid, M. (2019). A review on the selected applications of forecasting models in renewable power systems. *Renewable and Sustainable Energy Reviews*, *100*, 9–21. https://doi.org/10.1016/j.rser.2018.09.046

Bauer, P., Thorpe, A., & Brunet, G. (2015). The quiet revolution of numerical weather prediction. *Nature*, *525*(7567), 47–55. https://doi.org/10.1038/nature14956

Bessa, R. J., Möhrlen, C., Fundel, V., Siefert, M., Browell, J., Haglund El Gaidi, S., Hodge, B.-M., Cali, U., & Kariniotakis, G. (2017). Towards improved understanding of the applicability of uncertainty forecasts in the electric power industry. *Energies*, *10*(9), 1402. https://doi.org/10.3390/en10091402

Bessa, R., & Matos, M. (2010). Comparison of probabilistic and deterministic approaches for setting operating reserve in systems with high penetration of wind power. *7th Mediterranean Conference and Exhibition on Power Generation, Transmission, Distribution and Energy Conversion (MedPower 2010)*. https://doi.org/10.1049/cp.2010.0867

Brown, T., Hörsch, J., & Schlachtberger, D. (2018). PyPSA: Python for Power System Analysis. *Journal of Open Research Software*. https://doi.org/10.5334/jors.188

Buller, C. (2023). *Optimizing energy dispatch utilizing uncertainty information in probabilistic forecasts* [Bachelor's Thesis]. Constructor University Bremen. https://elib.dlr.de/195357/

Conejo, A. J., & Baringo, L. (2017, December). Unit commitment and economic dispatch. In *Power electronics and power systems* (pp. 197–232). Springer International Publishing. https://doi.org/10.1007/978-3-319-69407-8_7

Conejo, A. J., Carrión, M., & Morales, J. M. (2010). Decision making under uncertainty in electricity markets. In *International series in operations research & management science* (pp. 1–26). Springer US. https://doi.org/10.1007/978-1-4419-7421-1_1

Denholm, P., & Mai, T. (2019). Timescales of energy storage needed for reducing renewable energy curtailment. *Renewable Energy*, *130*, 388–399. https://doi.org/10.1016/j.renene.2018.06.079

ENTSO-E. (2021). All TSOs Biennial Progress Report on Operational Probabilistic Coordinated Security Assessment and Risk Management. Retrieved October 30, 2023, from https://annualreport2021.entsoe.eu/system-operation/

ENTSO-E. (2022). European Resource Adequacy Assessment, Executive Report, Annex 2 and Annex 3. Retrieved October 30, 2023, from https://www.entsoe.eu/outlooks/eraa/2022/eraa-downloads/

Hirth, L., & Ziegenhagen, I. (2015). Balancing power and variable renewables: Three links. *Renewable and Sustainable Energy Reviews*, *50*, 1035–1051. https://doi.org/10.1016/j.rser.2015.04.180

Hofmann, F. (2023). Linopy: Linear optimization with n-dimensional labeled variables. *Journal of Open Source Software*, *8*(84), 4823. https://doi.org/10.21105/joss.04823

IEA. (2020). Power systems in transition – Challenges and opportunities ahead for electricity security – chapter 1. Retrieved October 30, 2023, from https://www.iea.org/reports/power-systems-in-transition

IEA. (2021). Net Zero by 2050 – Summary for policy makers. Retrieved October 30, 2023, from https://www.iea.org/reports/net-zero-by-2050

IEA. (2022). Steering Electricity Markets towards a Rapid Decarbonisation – Chapter 5. Retrieved October 30, 2023, from https://www.iea.org/reports/steering-electricity-markets-towards-a-rapid-decarbonisation

Klæboe, G., & Fosso, O. B. (2013). Optimal bidding in sequential physical markets — a literature review and framework discussion. *2013 IEEE Grenoble Conference*, 1–6. https://doi.org/10.1109/PTC.2013.6652371

Koch, C., & Hirth, L. (2019). Short-term electricity trading for system balancing: An empirical analysis of the role of intraday trading in balancing germany's electricity system. *Renewable and Sustainable Energy Reviews*, *113*, 109275. https://doi.org/10.1016/j.rser.2019.109275

Kraft, E., Russo, M., Keles, D., & Bertsch, V. (2023). Stochastic optimization of trading strategies in sequential electricity markets. *European Journal of Operational Research*, *308*(1), 400–421. https://doi.org/10.1016/j.ejor.2022.10.040

Leutbecher, M., & Palmer, T. N. (2008). Ensemble Forecasting. *Journal of Computational Physics*, *227*(7), 3515–3539. https://doi.org/10.1016/j.jcp.2007.02.014

Morales, J. M., Zugno, M., Pineda, S., & Pinson, P. (2014). Electricity market clearing with improved scheduling of stochastic production. *European Journal of Operational Research*, *235*(3), 765–774. https://doi.org/10.1016/j.ejor.2013.11.013

Pinson, P. (2023). What may future electricity markets look like? *Journal of Modern Power Systems and Clean Energy*, *11*(3), 705–713. https://doi.org/10.35833/mpce.2023.000073

Schyska, B. U. (2021). *Coaction of input parameters and model sensitivities in numerical power system modeling* [Doctoral dissertation, Universität Oldenburg].

Sweeney, C., Bessa, R. J., Browell, J., & Pinson, P. (2019). The future of forecasting for renewable energy. *WIREs Energy and Environment*, *9*(2). https://doi.org/10.1002/wene.365

Theuer, F., van Dooren, M. F., von Bremen, L., & Kühn, M. (2020). Minute-scale power forecast of offshore wind turbines using long-range single-doppler lidar measurements. *Wind Energy Science*, *5*(4), 1449–1468. https://doi.org/10.5194/wes-5-1449-2020

Victoria, M., Zhu, K., Zeyen, E., & Brown, T. (2023). Pypsa technology data base. Retrieved October 29, 2023, from https://technology-data.readthedocs.io/en/latest/

Wilks, D. S. (2019). Chapter 4 - parametric probability distributions. In D. S. Wilks (Ed.), *Statistical methods in the atmospheric sciences* (4th ed., pp. 77–141). Elsevier. https://doi.org/10.1016/B978-0-12-815823-4.00004-3

Zheng, Q. P., Wang, J., & Liu, A. L. (2015). Stochastic optimization for unit commitment—a review. *IEEE Transactions on Power Systems*, *30*(4), 1913–1924. https://doi.org/10.1109/tpwrs.2014.2355204

Zhou, Z., Botterud, A., Wang, J., Bessa, R., Keko, H., Sumaili, J., & Miranda, V. (2012). Application of probabilistic wind power forecasting in electricity markets. *Wind Energy*, *16*(3), 321–338. https://doi.org/10.1002/we.1496

Declaration of Authorship

Family Name, First Name	Bents, Hauke Mirco
Matriculation number	6419347
Kind of thesis	Master

English

I hereby declare in lieu of an oath that I have written this thesis independently and have not used any sources or aids other than those specified. I also declare that I have followed the general principles of scientific work and publication as laid down in the guidelines of good scientific practice of the Carl von Ossietzky University of Oldenburg.

German

Hiermit versichere ich an Eides statt, dass ich diese Arbeit selbstständig verfasst und keine anderen als die angegebenen Quellen und Hilfsmittel benutzt habe. Außerdem versichere ich, dass ich die allgemeinen Prinzipien wissenschaftlicher Arbeit und Veröffentlichung, wie sie in den Leitlinien guter wissenschaftlicher Praxis der Carl von Ossietzky Universität Oldenburg festgelegt sind, befolgt habe.

Oldenburg, 21st November 2023

Hauke Bents